

INVESTIGATING MOTILITY PERFORMANCE OF *BATRACHOCHYTRIUM*  
*DENDROBATIDIS* ZOOSPORES AND ITS ASSOCIATION WITH  
MITOCHONDRIAL DENSITY AND PATHOGENICITY

by

Devlin B. Jackson, B.A.

A thesis submitted to the Graduate Council of  
Texas State University in partial fulfillment  
of the requirements for the degree of  
Master of Science  
with a Major in Biology  
May 2020

Committee Members:

David Rodriguez, Chair

Dittmar Hahn

Camila Carlos-Shanley

**COPYRIGHT**

by

Devlin B. Jackson

2020

## **FAIR USE AND AUTHOR'S PERMISSION STATEMENT**

### **Fair Use**

This work is protected by the Copyright Laws of the United States (Public Law 94-553, section 107). Consistent with fair use as defined in the Copyright Laws, brief quotations from this material are allowed with proper acknowledgement. Use of this material for financial gain without the author's express written permission is not allowed.

### **Duplication Permission**

As the copyright holder of this work I, Devlin B. Jackson, authorize duplication of this work, in whole or in part, for educational or scholarly purposes only.

## **DEDICATION**

My mother Marilyn S. Jackson and my wife Valerie Zurcher

## ACKNOWLEDGEMENTS

I would like to thank a number of people without whom I would not have been able to complete this thesis. Firstly, I would like to thank my advisor and mentor Dr. David Rodriguez who patiently instructed and guided me through the master's program. I would also like to thank my other committee members Dr. Dittmar Hahn and Dr. Camilla Carlos-Shanley who have gifted me with their time and some constructive criticism. I am especially grateful to the Garcia lab for supplying me with osmium tetroxide and other reagents necessary for microscopy. Emely Weibe in particular guided me through several fixation and staining protocols and helped me troubleshoot. My lab mates in the Rodriguez lab Carlos Baca, Stephen Harding, Clarissa Rivera, Daniel Puckett Monica Argueta, for their moral support and numerous occasions for which they generously provided me with help. Thom Marshall taught me how to isolate and maintain chytrid cultures and provided most of the isolates that I used in this project. I thank Drs. Felipe Toldeo and Timothy James for providing a Brazilian isolate. I would like to thank the Hahn lab for the use of equipment and reagents and especially Trina Guerra for instructing me on dPCR protocol. Alyssa Savage and the ARSC staff provided me with training and access to the TEM and Confocal microscope. Dr. Koke's histology and cytology courses provided my introduction to advanced microscopy.

## TABLE OF CONTENTS

	<b>Page</b>
ACKNOWLEDGEMENTS.....	v
LIST OF TABLES .....	vii
LIST OF FIGURES .....	viii
LIST OF ABBREVIATIONS .....	x
ABSTRACT .....	xi
CHAPTER	
I. INTRODUCTION.....	1
II. METHODS.....	8
III. RESULTS .....	13
IV. DISCUSSION.....	16
LITERATURE CITED .....	48

## LIST OF TABLES

<b>Table</b>	<b>Page</b>
1. The dPCR results of -mtSNP count per zoospore equivalent are summarized in the table below .....	19
2. Average mitochondrial counts and maximum and minimum observed numbers for six isolates are displayed below along with the number of zoospores in each sample ....	19
3. The average zoospore velocity from the confocal time series micrographs are summarized in the table below .....	19

## LIST OF FIGURES

Figure	Page
1. The dPCR results from the mtSNP protocol are represented by a bar graph indicating the number of copies of mtSNP Bdmt26360 per $\mu\text{l}$ of reaction volume for each of the identified isolates .....	20
2. A Confocal Micrograph of a <i>Bd</i> zoospore stained with MitoView™ Green displays two bright clusters of mitochondria in the lower right hand corner of the image .....	20
3. A confocal micrograph of a <i>Bd</i> zoospore stained with MitoView™ Green displays two purple clusters of mitochondria in the center of the image.....	21
4. This box plot indicates zoospore motility performance in $\mu\text{m/s}$ with TXST015 being the fastest and TXST002 being the slowest.....	21
5. This box plot of TEM observations of mitochondria in <i>Bd</i> zoospores indicates that the greatest variation in the number of mitochondria observed was in TXST011 which had the instances of both greatest and least .....	22
6. A Scatter plot of zoospore motility vs TEM mitochondrial observations does not indicate any correlation between the two variables. ....	22
7. A Scatter plot of SNP copy number vs. average mitochondrial density from TEM images has been plotted with the SNP copy numbers obtained from dPCR and the $R^2$ value is displayed on the graph. ....	23
8. A box plot of qPCR results for pre-inoculation and postmortem swabs measured in zoospore equivalents with t-tests between treatment groups for times 1, 2, and 3 is displayed above.....	23
9. The mortality curve for the <i>Acris crepitans</i> infection experiment is flat with no indication of increased mortality due to the presence of a pathogen.....	24
10. TEM Micrographs of <i>Bd</i> Zoospores with scale bar in the lower left corner and mitochondria circled in red are labeled with isolate identification number followed by an underscore and a number which corresponds to the original image file.....	25
11. A confocal time series of micrographs of live <i>Bd</i> zoospores which are identified by isolate_image file name_sequence number are displayed above.....	38

## LIST OF ABBREVIATIONS

<b>Abbreviation</b>	<b>Description</b>
EIDs	Emerging Infectious Diseases
<i>Bd</i>	<i>Batrachochytrium dendrobatidis</i>
µm	Micrometer
Cm	Centimeter
°C	Degrees Celsius
GPL	Global Panzootic Lineage
ITS1	Internal Transcribed Spacer One
qPCR	Quantitative Polymerase Chain Reaction
SNP	Single Nucleotide Polymorphism
dPCR	Digital Polymerase Chain Reaction
TEM	Transmission Electron Microscopy
FCS	Fetal Calf Serum
DMSO	Dimethyl Sulfoxide
rcf	Relative Centrifugal Force
ETOH	Ethanol Alcohol
DI	Deionized
ZS	Zoospore
z.e.	Zoospore Equivalent

## ABSTRACT

Chytridiomycosis, an emerging infectious disease caused by *Batrachochytrium dendrobatidis* (*Bd*), has spread globally and demonstrates high genetic diversity amongst multiple strains. I investigated the use of a mitochondrial SNP in a digital PCR assay to evaluate the variance in copy number between isolates and compare it to a qPCR assay that is the current standard protocol for determining pathogen load of *Bd* on host amphibians. I also tested for differences in mitochondrial density in Texas isolates using TEM and confocal microscopy. Furthermore I used a timed series of images taken with the confocal to compare zoospore motility performance of between isolates. To determine if susceptibility differs between strains of *Bd* isolated from Texas with differing motility performance, I conducted an infection experiment on twenty-seven northern cricket frogs (*Acris crepitans*). The frogs were divided into two experimental groups (n = 10 in each) and one control group (n = 7). The two experimental groups were each inoculated twice with local *Bd* isolates TXST002 and TXST015 (*Bd*GPL) and a third time with isolate BAF038 (*Bd*ASIA-2/*Bd*BRAZIL). My results show that *Acris crepitans* is highly resistant to chytridiomycosis, which indicates that they may serve as potential *Bd* super-spreader in the wild.

## I. INTRODUCTION

The loss of biodiversity on a global scale is currently of great international concern. Emerging infectious diseases (EIDs) of wildlife have significant impacts on biodiversity, habitat, and human health (Daszak, Cunningham et al. 2000). Amphibians have long been considered indicator species for the overall environmental health of their habitat (Blaustein and M. Kiesecker 2002). While many of the population declines and extinctions that we see in amphibian populations today can be attributed to the complex interaction of factors such as habitat loss, introduction of nonnative species, pollution, environmental contaminants, increased UV exposure, and climate change, other declines and mass mortality events were unexplained prior to the 1998 mass mortality event in a colony of poison dart frogs at the National Zoo in Washington D.C. (DePaula and Catão-Dias 2011). This event provided the first bit of evidence that a hereto undescribed chytrid fungi was the etiological agent behind the mysterious amphibian population declines (Longcore, Pessier et al. 1999). Chytridiomycosis an emerging infectious disease (EID) caused by the fungus *Batrachochytrium dendrobatidis* (*Bd*) has since been identified as a prime factor in population declines and extinctions of hundreds of amphibian species around the world (Stuart, Chanson et al. 2005, Skerratt, Berger et al. 2007). Global amphibian populations are declining and have been for several decades (Houlahan, Findlay et al. 2000). In 2013, 1,240 of the 6,996 known amphibian species were tested and 42% were positive for *Batrachochytrium dendrobatidis* (*Bd*) infections (Olson, Aanensen et al. 2013). Chytridiomycosis is characterized by the invasion of amphibian skin by *Bd*, which causes *hyperkeratosis*, osmotic imbalance, and frequently death by cardiac arrest (Berger, Speare et al. 1998, Voyles, Young et al. 2009).

The amphibian-killing fungus, first described by (Longcore, Pessier et al. 1999), is a Eukaryote in the Kingdom *Fungi*, Phylum *Chytridiomycota*, Class *Chytridiomycetes*, Order *Rhizophydiales* (Longcore, Pessier et al. 1999). There are several hundred described species of chytrid fungi, most of which are saprobes living on decomposing organic substrates. *Bd* is the first chytrid fungus known to attack living vertebrate hosts (Daszak, Cunningham et al. 2000). Its zoospores are motile and mostly spherical or ovate in shape ranging from 3-5  $\mu\text{m}$  in diameter (Longcore, Pessier et al. 1999). Upon release from a zoosporangium the zoospores may become somewhat elongate (Longcore, Pessier et al. 1999). Zoospores can have between one and many cytoplasmic extensions and have a posterior flagellum that ranges from 19-20  $\mu\text{m}$  (Longcore, Pessier et al. 1999). Lipid globules, microbodies and aggregations of ribosomes can be observed using phase microscopy. Zoospores develop into germlings which produce fine thread-like rhizoids from either a single location or several locations as the germling grows into a zoosporangium over the course of four to five days (Longcore, Pessier et al. 1999). Rhizoids may be short and bushy or long and branched (Longcore, Pessier et al. 1999). Once mature, the zoosporangium will have one to several discharge papillae. The discharge papillae, formed during the growth of the zoosporangium, have walls that form plugs at the tip of the papillae which will deliquesce releasing fresh zoospores. Sporangia can range from 20-40 $\mu\text{m}$  in diameter (Longcore, Pessier et al. 1999).

The *Bd* life cycle has two primary stages, 1: A short-lived free-swimming motile zoospore which is used for dispersal, and 2: sessile monocentric thalli that develop into zoosporangia for asexual reproduction (Berger, Marantelli et al. 2005). The contents inside of the zoosporangium divide into new zoospores that leave the structure by way of

one or more papillae (Berger, Marantelli et al. 2005). Sexual reproduction of *Bd* has not been observed. The only deviation from the above life cycle occurs when more than one zoosporangium develops from a single zoospore, this is known as colonial development (Longcore, Pessier et al. 1999). The cycle remains the same regardless of whether the organism is cultivated or growing in amphibian skin. The life duration in vitro is 4-5 days at 22°C, the same is assumed to be true of amphibian skin, but this has not been verified (Berger, Marantelli et al. 2005). The zoosporangium will remain empty following the departure of the zoospores, but its chitinous wall may persist as an empty shell and is often colonized by bacteria (DePaula and Catão-Dias 2011).

Zoospore movement is one mechanism that enables *Bd* to move rapidly among and within populations (Olson, Aanensen et al. 2013). *Bd* zoospore motility may play a role in the establishment and progression of chytridiomycosis (Berger, Hyatt et al. 2005). Positive chemotaxis of *Bd* towards various nutrient sources (Moss, Reddy et al. 2008) and negative chemotaxis away from antifungal compounds has been demonstrated (Lam, Walton et al. 2011). One study examined the duration of motility and distance traveled by zoospores, they found that 50% of zoospores settled and encysted within 18 hours and 95% within 24 hours, they also observed that the majority of zoospores moved no more than 2 cm (Piotrowski, Annis et al. 2004).

*Bd* exhibits high genetic diversity, with many isolates demonstrating significant genetic differences from others and some showing geographic associations (Rosenblum et al. 2013). Two divergent lineages of note are the *Bd*-GPL (Global Panzootic Lineage), which is associated with massive amphibian population declines and *Bd* Brazil which is not associated with amphibian population declines (Becker, Greenspan et al. 2017). *Bd*

GPL and *Bd* Brazil have been shown to have overlapping geographical ranges (Jenkinson, Rodriguez et al. 2018). ITS1 regions with varying copy numbers are routinely used as the standard marker for DNA-based identification of Fungi. This region has also been used to quantify fungal pathogen loads and to determine prevalence (E Smith, Douhan et al. 2008). Longo et al. (2013) found copy numbers of ITS1 that ranged from 10-144 in eight strains of *Bd* and Kirshtein et al. (2008) found a strain with 169 copies. This broad range of copy number has resulted in both over and under estimations of prevalence and pathogen load when using the Boyle et al. (2014) qPCR protocol (Longo, Rodriguez et al. 2013, Rebollar, Woodhams et al. 2017). To compound the difficulties of determining infection intensity, anurans can be infected with more than one strain of *Bd* both of which will have multiple copies of the ITS1 region (Rodriguez, Becker et al. 2014).

Chytridiomycosis infection intensity thresholds of 10,000 zoospores or *Bd* genomic equivalents have been associated with disease, mortality, and population decline. However, some species infected with much lower (10 fold) infection intensity have also experienced high rates of mortality and population declines (Rebollar, Woodhams et al. 2017). This is likely explained by the use of a Real-Time qPCR TaqMan assay developed by Boyle et al. 2004, that relies on the use of standards, which are biased due to variation in the ITS1 copy number within and between strains (Longo, Rodriguez et al. 2013). AAHL98, the strain used by Boyle et al. (2004) to develop the qPCR assay that is currently being used to determine both prevalence and infection load, was thought to have 10 copies of the ITS1 5.8S ribosomal gene (Boyle, Boyle et al. 2004). Longo et al. (2013) demonstrated that variations in copy number between the

reference strain and the field strain can impact pathogen load estimate by as much as two orders of magnitude. For example, if the ITS1 copy number of the reference strain is higher than that of the field isolate then the intensity of infection will be underestimated, and when the ratio is reversed then intensity values will be overestimated (Rebollar, Woodhams et al. 2017).

*Bd* infection occurs when the monoflagellated free-swimming zoospores recently shed into the water or other substrate by a zoosporangium on an infected individual come into contact with another potential amphibian host (Longcore, Pessier et al. 1999, Berger, Marantelli et al. 2005). The zoospore will burrow down several layers into the skin to where keratin is produced (Kolby and Daszak 2016). The zoospores will then remain there growing and developing from zoospore to germling to zoosporangia where through mitotic division more zoospores are produced asexually (Kolby and Daszak 2016). If the animal is in an aquatic environment the spores are released into the water, however if the animal is in a terrestrial environment the zoospores will likely reinfect that animal resulting in a heavier pathogen load (Kolby and Daszak 2016). An amphibian infected with *Bd* can experience a set of symptoms ranging from asymptomatic to death by chytridiomycosis (Berger, Marantelli et al. 2005). Susceptible individuals when infected by *Bd* experience hyperkeratosis and abnormal shedding, which interferes with the animal's osmoregulation and ability to maintain electrolyte balance (Kolby and Daszak 2016). Other histopathological findings include hyperplasia and focal necrosis of epidermal cells along with occasional ulcerations associated with bacteria in areas of keratin accumulation and empty zoosporangia (DePaula and Catão-Dias 2011). Lesions frequently occur on the ventral abdomen, pelvis, legs and toes (DePaula and Catão-Dias

2011). In severe cases this leads to death by cardiac arrest (Voyles, Young et al. 2009). Other behaviors may be exhibited by infected animals such as lethargy, anorexia, and loss of righting reflex but these observations are inconsistent and nonspecific and thus are not diagnostic tools (DePaula and Catão-Dias 2011, Kolby and Daszak 2016). The same is true for skin lesions making diagnosis in the field difficult to impossible (Kolby and Daszak 2016). Many amphibians have a defense system associated with their skin that provides protection from predation and pathogenic microorganisms. Rollins-Smith et al. (2001) demonstrated that six peptides derived from three species of amphibian were able to inhibit the growth of *Bd*. This suggests that understanding this mechanism may be important to conservation efforts.

Distinctions between presence of *Bd*, infection by *Bd* and the disease chytridiomycosis are important as each is indicative of a different state of physical presence by the pathogen (Kolby and Daszak 2016). Currently presence can be determined by using a skin swab and then running the Boyle et al. (2004) quantitative PCR protocol, which is highly specific and sensitive although it may in some cases over or under report presence. However, presence alone will not determine the state of infection. In order to confirm infection or determine diseased state tissue sampling and histological examination are required (Skerratt, Mendez et al. 2011). Disease is indicated by clinical signs of detriment to tissues bordering *Bd* infection sites. It is possible for an animal to be infected but not diseased (Skerratt, Mendez et al. 2011).

*Acris crepitans* commonly known as the Northern Cricket Frog is unusual in that they are fairly short lived. They have an average life span of only four months with a complete population turn over in 16 months. They have a wide geographical range from

New York to West Texas and even North Dakota. Populations in the northern reaches of their range are in decline (Lehtinen and MacDonald 2011).

An assay targeting a region with significantly less variation in copy number that is capable of determining prevalence and pathogen load from field samples would help standardize *Bd* data moving forward. Comparison of standardized data would help determine which strains are most virulent and would allow conservationists to focus on populations that are at the greatest risk. I wanted to determine if a mitochondrial SNP would have a lower copy number variation between strains in order to develop a better assay using dPCR. Additionally, I was curious to what extent the number of mitochondria possessed by a zoospore would correlate with the velocity of the zoospore's motility. Finally, I investigated if either mitochondrial number or motility performance correlated with increased pathogenicity via an infection experiment using *A. crepitans* comparing two isolates with different motility performance.

## II. METHODS

The development of a digital PCR (dPCR) assay to create a reference standard independent of ITS1 copy number variation using a mitochondrial DNA sequence with a SNP rather than ITS1 and combined with zoospore counts could assist in the cross comparison of differing studies and help produce more accurate estimates of prevalence and pathogen load. I attempted to test the protocol using nine Texas isolates (GPL) and one well characterized isolate from Panama (JEL423), ALKL2 from Virginia, USA, and a *Bd Asia2/BdBrazil* strain. I used TEM micrographs of zoospores from each isolate to estimate the number of observable mitochondria per zoospore to compare with the dPCR assay. The confocal was also used to test zoospore motility performance by running timed series of micrographs and to determine the velocity of individual zoospore. Lastly an infection experiment was run using *A. crepitans* as a host to test for differences in pathogenicity and infectivity of two isolates with differing levels of motility performance.

### **Isolation and Quantification**

Tadpoles were collected from ponds with a net and were transported to the lab in water from the collection site. Collected tadpoles were euthanized by decapitation with a razor blade. The keratinized mouth parts including the upper and lower jaw sheaths and denticles were removed by dissection under a microscope. The tissues were then separated and placed onto a 1% tryptone agar plate with streptomycin and penicillin (250mg/L). Each piece of tissue was dragged across the plate through the agar with a hypodermic needle to remove bacteria and debris. This procedure was repeated with three plates and then the tissues were placed onto a 1% tryptone agar plate with no antibiotics and incubated at 20°C until chytrid were observed (Longcore, Pessier et al. 1999). Once

chytrids were observed, the plates were sub-cultured, isolates were genotyped, and each was cryopreserved in filter sterilized fetal calf serum solution (40 ml .45µm filtered 1% tryptone broth, 5ml DMSO and 5 ml .45µm filtered FCS) at -80C° (Marshall, Baca et al. 2019).

Eleven unique isolates were taken from cryo-storage and revived in 1% tryptone broth in 50ml tissue culture flasks. The isolates were allowed to grow for 1-2 weeks and then filtered with a 10 µm syringe in order to obtain zoospores of the same age and state of development. In a 50 ml tissue culture flask, 1 ml of the filtered zoospore solution was placed in 9 ml of 1% tryptone broth and incubated at room temperature in the dark for 4-6 days. The zoospores were then filtered again with a 10 µm filter and counted using a hemocytometer and microscope. Dilutions of  $1 \times 10^6$  zoospores were prepared in 1.5 ml Eppendorf tubes. The tubes were spun down at 21130 rcf for 10 min and the supernatant was removed. The samples were then placed in a speedvac centrifuge on medium heat and low vacuum until dry. After drying the samples were placed in a -4°C freezer until DNA Extraction. Extraction was performed using a PrepMan solution (Applied Biosystems, Inc.), thus 100µl of PrepMan was placed in each tube containing  $1 \times 10^6$  dry zoospores and then incubated at 100°C for 10 min. After incubation the samples were spun down at 21130 rcf for 10 min and then 80 µl of supernatant was removed. The samples were then placed in the -4°C freezer.

### **Digital PCR**

PCR reactions loaded into the dPCR chips (QuantStudio 3D Digital Chip Kit v2) were carried out using 0.725 µl of a custom TaqMan genotyping assay (Bdmt26360) sourced from Life Technologies, Inc. (Jenkinson et al. 2018), 7.25 µl of 3D Digital PCR

Master Mix v2 (Applied Biosystems, Inc.), 5.525  $\mu$ l of nuclease-free water, and 1  $\mu$ l of template. Thermocycling was performed on a dual-flat block Proflex PCR system (Applied Biosystems, Inc.). Each reaction was run in triplicate for each extraction of  $1 \times 10^6$  zoospores. The data were analyzed for copy number variation using online QuantStudio 3D AnalysisSuite Cloud Software (ThermoFisher, Inc). Each strain was then compared to see if there was a uniform copy number of the SNP locus.

### **Microscopy**

A pellet of *Bd* was incubated in 2.5% glutaraldehyde for 2 hours. Next, the cells were washed twice in 0.05M cacodylate (800 rcf 10 min) and then stained with osmium tetroxide for 2 hours then centrifuged at 1500 rcf for 10 min. The pellet was washed 2 times in 0.05M cacodylate (1500rcf 10 min). Dehydration was then performed with 30%, 50%, 70%, and 95% ETOH with a 15-minute immersion in each solution before being centrifuged again at 800 rcf for 10 minutes. The pellet was then placed in LR white and incubated for 1 hour before being centrifuged for 10 minutes at 800 rcf after which the LR white was removed. The pellet was then transferred to a gelatin capsule and then covered in LR white. The capsule and pellet were then placed in an oven at 65°C for 24hrs. Once out of the oven the gelatin capsule was cut away and the stained pellet was exposed. The sample was then sectioned on an ultramicrotome and mounted on a #400 mesh copper grid for viewing on the JEM-1200EXII-1 TEM. Images were obtained using an Orius CS1000 CCD camera. The images were viewed in iPhoto and mitochondria were identified by the distinguishing characteristics of cristae and were circled in red with the iPhoto editing software (Figures 10.1-10.82).

An Olympus FV1000 confocal laser scanning biological microscope was used to image zoospores stained with MitoView™ Green. Cells were harvested 4 days after inoculation by flooding the plates with 1% tryptone broth. The zoospores were centrifuged at 500 rcf. In a darkroom the pellet was mixed into a 100 nM solution of MitoView™ Green and DI water. The solution was incubated for 30 minutes at room temperature. Next the solution was centrifuged gently at 500 rcf for 10 minutes. The supernatant was removed, and the pellet was transferred to a slide and placed in glycerol before a cover slip was set in place with nail polish. Lasers excitation/emission spectrum was set at 490/523nm (MitoView™ Green). Images were obtained using Fluoroview software.

Cells were harvested in the same manner as above but were not concentrated into a pellet. Instead they were kept in a solution of 1% tryptone broth. Next the cells were placed on a slide with a shallow well and a slipcover. They were viewed using the Olympus FV1000 at 200x power. A one-minute timed series was run using the Fluoroview software. The images were viewed frame by frame and the velocity of the zoospore was calculated using the scalebar feature the time lapse of 2.18052s/frame (Figures 11.1-11.57). These data were compared with mitochondrial counts obtained from the TEM imaging.

### **Infection experiment**

*Acris crepitans* (n = 27) were collected from the Clear Fork of the Brazos (32.808646, -99.604112) and swabbed to determine infection state prior to inoculation. The Cricket frogs were divided into two experimental groups (n = 10) and one control group (n = 7). Each individual was placed into sterile 50ml falcon tubes with 10 ml of

water. The two experimental groups had  $2 \times 10^6$  zoospores of isolates TXST015 (17.55  $\mu\text{m/s}$ ) and TXST002 (7.41  $\mu\text{m/s}$ ), respectively, in with the 10 mL of autoclaved DI water. These were chosen because they represent the fastest and slowest of the TXST isolates. After 24 hrs., all of the frogs were moved to individual shoebox sized clear plastic terrariums with a small amount of sphagnum moss on one end and a petri dish filled with the original 10 ml of water from the falcon tube plus an additional 25 ml of autoclaved DI water. The water was changed on the 4<sup>th</sup> day following inoculation. All of the terrariums were kept in a 19 C° incubator on a 12 on/12 off light cycle. The water was changed every 3-4 days and the frogs were fed 3-5 crickets every time the water was changed. 23 days after the initial inoculation I inoculated again with  $20 \times 10^6$  zoospores using the same methodology and the same isolates. 32 days later the frogs were inoculated a third time with  $20 \times 10^6$  zoospores from isolate BAF038 a *Bd* Asia2/Brazil strain. The experiment was terminated 12 days after the third inoculation. Time of death post inoculation was recorded and swabs were collected before each inoculation and after each death. Swabs were tested for *Bd* using the Boyle et al. (2004) protocol with standards of genomic equivalents ranging from 0.1 – 1000 zoospores.

### III. RESULTS

#### dPCR

SNP number does vary between isolates from 75-275 SNP's per 1.0  $\mu\text{L}$  of dPCR reaction volume (Figure 1). TM26 has between 200 and 225 copies of the SNP per 1.0  $\mu\text{L}$  of reaction volume and  $10000\text{ZS}/14.5 \mu\text{L reaction volume} = 690\text{ZS}/\mu\text{L}/225\text{SNP}/\mu\text{L}$   $\text{RXN}=3.06\text{SNP}/\text{ZS}$  (Table 1). Significant variation in the number of mitochondria combined with variations in the copy number of the SNP region amongst isolates rendered this line of inquiry moot.

#### Mitochondrial Counts

I was able to successfully stain mitochondria using the MitoView™ Green. However, it proved to be beyond the capabilities of the instrument to render them with sufficient resolution to count. Most images displayed between 1 and 3 brightly fluorescent regions which I believe to be clusters of mitochondria that are too small and close to be distinguished from one another. Figures 2 and 3 both show small bright clusters of mitochondria.

Table 2 contains the mitochondrial counts obtained from TEM micrographs of zoospores. Mitochondria were counted for isolates TXST002 (n = 25), TXST015 (n = 26), TXST011 (n = 16), TXST035 (n = 7), TXST036 (n = 6) and JEL423 (n = 7). The average number of mitochondria observed for TXST002 was 5.84, the maximum was 13 and the minimum was 1. For TXST015 the average was 4.34, the maximum 10 and the minimum was 2. TXST011 had an average count of 10.31, a maximum of 33 and a minimum of 1. The average number of mitochondria observed in TXST035 was 5.86, the maximum was 8 and the minimum was 3. The average number of mitochondria observed

in TXST036 was 5.33, the maximum was 7 and the minimum was 3. The average number of mitochondria observed in JEL423 was 11.4, the maximum was 19 and the minimum was 5. A two tailed t test between the mitochondrial count numbers of TXST002 and TXST015 had a P value of 0.0389 indicating significant statistical difference was observed between the two isolates (Figure 5).

### **Zoospore Performance**

Motility measurements for seven isolates, TXST002 (n = 32), TXST011 (n = 30), TXST006 (n = 44), TXST007 (n = 20), TXST015 (n = 32), TXST032 (n = 7), and TXST036 (n = 7) are summarized in (Table 3). Isolate TXST002 averaged 8.48  $\mu\text{m/s}$ , TXST06 averaged 13.12  $\mu\text{m/s}$ , TXST007 averaged 5.83  $\mu\text{m/s}$ , TXST011 averaged 9.83  $\mu\text{m/s}$ , TXST015 averaged 21.22  $\mu\text{m/s}$ , TXST032 averaged 7.80  $\mu\text{m/s}$ , and TXST036 averaged 9.02  $\mu\text{m/s}$ . A two-tailed T test between TXST002 velocities and TXST015 velocities, the slowest and fastest isolates respectively, returned a P value of  $1.21 \times 10^{-08}$ , which indicates a significant difference in motility performance between the two isolates. The fastest observed individual zoospore was from TXST015, which was recorded moving at 41.27  $\mu\text{m/s}$  (Figure 4). A scatterplot of zoospore velocity vs. TEM observations of mitochondria returned a regression line with a negative slope (Figure 6).

### **Pathogenicity and Infectivity**

The infection experiment began on 10/21/2019 and ran through 12/23/2019. During the first inoculation period on day six one individual in the control group died; although, this was most likely due to dehydration as the frog had become trapped between the lid and the terrarium. On November 30, 2019 during the second inoculation period an individual in the TXST015 group died but showed no signs of having

chytridiomycosis. Two individuals died on Dec 4, 2019, one from the TXST015 group and the other from the control group. An individual from the TXST015 group died on December 5, 2019. No frogs showed any obvious signs of having succumbed to chytridiomycosis. No frogs died following the third inoculation. A qPCR test on the swabs indicated that both experimental groups had individuals with pathogen loads well in excess of 10,000 z.e. following the second inoculation. The TXST002 experimental group had very low to no indication of *Bd* presence at the completion of the experiment, with the exception of one individual who had a pathogen load of around 25,000 z.e. The TXST015 group was heavily infected with one individual carrying a load of over 70,000 z.e. Tests on the frogs that died during the experiment showed no signs of *Bd* presence. A t-test between Treatment 1 loads for both experimental groups returned a P-value of 0.386 indicating no statistical difference. A t-test between Treatment 2 loads for both experimental groups returned a P-value of 0.3769 indicating no statistical difference. A t-test between treatment 3 loads for both experimental groups returned a P-value of 0.1886 indicating no statistical difference (Figure 8). The mortality curve show in (Figure 9) is relatively flat providing no indication of pathogen associated mortality (i.e., pathogenicity).

#### IV. DISCUSSION

The dPCR protocol utilizing the mitochondrial SNP (Bdmt26360) tested on 11 isolates indicated variations in the SNP copy number per zoospore that ranged from 2.5-9.2, an almost 4-fold difference (Figure 1). This copy number variation is not nearly as great as the variation found in between the ITS1 copy number variation between isolates utilizing the Boyle et al. (2004) protocol, but since data were collected from only 11 isolates, most of which are from the same geographical region, additional data collection utilizing more diverse sampling might result in increased copy variation. A correlation between the number of mitochondria observed in TEM images and SNP copy number per zoospore is apparent in Figure 7. Presently the need for the development of a stable metric to accurately quantify pathogen load between different isolates and strains of *Bd* remains an area of active investigation.

Utilizing the confocal with the MitoView™ Green stain proved to be a poor method for quantifying mitochondrial numbers within zoospores. While the staining was successful the resolution was not sufficient to identify and enumerate individual mitochondria. It may be possible to quantify the amount of fluorescence in zoospore micrographs using Image J. Data collected in this manner could prove to be a useful tool in the quantification of mitochondria within individual zoospores. TEM proved to be a better method for the quantification of mitochondria within *Bd* zoospores.

The primary difficulties encountered with TEM were inconsistent results with staining, equipment malfunctions, and analysis of micrographs. Many samples seemed to resist staining by osmium, and it was only by post staining with uranyl acetate that the cells became visible under low power. Often many features were indistinguishable until

after an image had been taken with the digital camera which made focusing very challenging. Many of the TXST015 micrographs contain images of zoospores with deteriorated plasma membranes which may indicate that the counts are low due the possibility of mitochondria having moved out of the cell. The glass knife maker in the ARSC lab was replaced in the middle of this project with a new Leica model and sections cut on that ultramicrotome were significantly improved which resulted in better image quality. Cristae were the feature used to identify mitochondria. Extreme morphology variations seem to be common amongst mitochondria within *Bd*. TEM micrographs represent a two-dimensional slice that is only 70nm thick providing an image that is far from complete. A scope and CNC ultramicrotome capable of sectioning, imaging and compiling a z stack would be useful in determining exact mitochondrial counts within zoospores. While mitochondrial counts within cells can vary drastically and change rapidly over short periods of time, harvesting zoospores 4-5 days after the inoculation of media and filtering by size should produce cultures that contain comparable populations.

A two tailed T-test between the mitochondrial counts of TXST002 and TXST015 suggests that there was no significant difference in the data sets. Continued investigation into the variation of mitochondrial density between isolates and strains could prove to worthwhile if a correlation between mitochondrial count and pathogenicity or motility performance can be established.

The motility performance experiment performed using the timed series feature on the Olympus FV1000 at 200x power worked very well. Analysis was straight forward using the FV1000 software. Initial experimentation with a haemocytometer resulted in not enough vertical space for zoospores to move around. This was solved by switching to

a slide with a shallow well. The limitations imposed by the 2.18052s intervals between images were not a significant impediment in the interpretation of zoospore movement, but continuous video imaging would eliminate the possibility of incorrectly tracing zoospore movement. While this study sought to link zoospore velocity to pathogenicity another potential avenue of investigation would be to look for an association with how far zoospores from differing isolates travel or how long they are capable of remaining motile to pathogenicity.

*Acris crepitans* was selected as the experimental host for this study based on their wide scale prevalence and tolerance to captivity and large local populations. Of the 27 individuals captured five died. Two of the five frogs that died were in the control group. None of the deceased frogs showed any signs of having chytridiomycosis. Of particular interest is the lack of *Bd* presence in the TXST002 experimental group at the termination of the experiment. One possible explanation is that there was competitive inhibition between the TXST002 and BAF038 isolates. Competitive inhibition between *Bd* isolates has not been the focus of rigorous investigation. Another possibility is that the TXST002/BAF038 coinfection triggered the production of antifungal peptides which cleared the infection whereas the other coinfection did not. *Acris crepitans* demonstrated a strong resistance to chytridiomycosis by *Bd* infection. This suggests that like the American Bullfrog (*Lithobates catesbeianus*), *Acris crepitans* has the potential to be a super spreader. The very large geographical range of *Acris crepitans* further suggest that this species is capable of contributing to the rapid spread of *Bd* within North America.

**Table 1. The dPCR results of -mtSNP count per zoospore equivalent are summarized in the table below.**

Isolate	TM26	TM28	TM30	TM33	TM36	TM39	TM88	TM91	TM127	ALKL2	JEL423
SNP/ZS	3.0	9.2	6.9	6.9	3.5	2.5	3.9	4.6	3.6	3.6	9.2

**Table 2. Average mitochondrial counts and maximum and minimum observed numbers for six isolates are displayed below along with the number of zoospores in each sample.**

Isolate	TXST002	TXST015	TXST011	TXST035	TXST036	JEL423
Average Mitochondrial Count	5.84	4.34	10.31	5.86	5.33	11.43
Maximum	13	10	33	8	7	19
Minimum	1	2	1	3	3	5
Sample Size	26	26	16	7	6	7

**Table 3. The average zoospore velocity from the confocal time series micrographs are summarized in the table below.**

Isolate	TXST002	TXST015	TXST011	TXST006	TXST007	TXST036	TXST032
Average velocity $\mu\text{m/s}$	8.48	21.22	9.83	13.12	5.83	9.02	7.80
Sample size	32	32	30	44	20	7	7

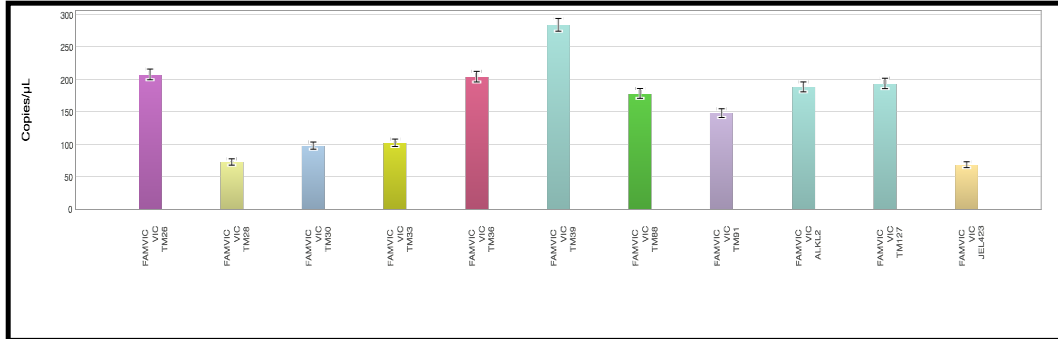


**Figure 1.** The dPCR results from the mtSNP protocol are represented by a bar graph indicating the number of copies of mtSNP Bdmt26360 per µl of reaction volume for each of the identified isolates.



**Figure 2.** A Confocal Micrograph of a *Bd* zoospore stained with MitoView™ Green displays two bright clusters of mitochondria in the lower right hand corner of the image.

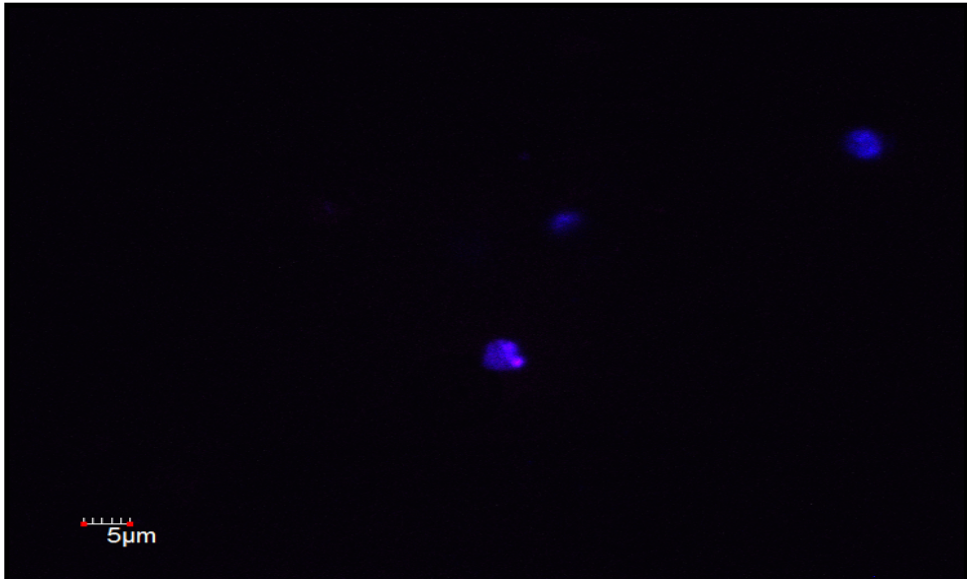


**Figure 3.** A confocal micrograph of a *Bd* zoospore stained with MitoView™. Green displays two purple clusters of mitochondria in the center of the image.

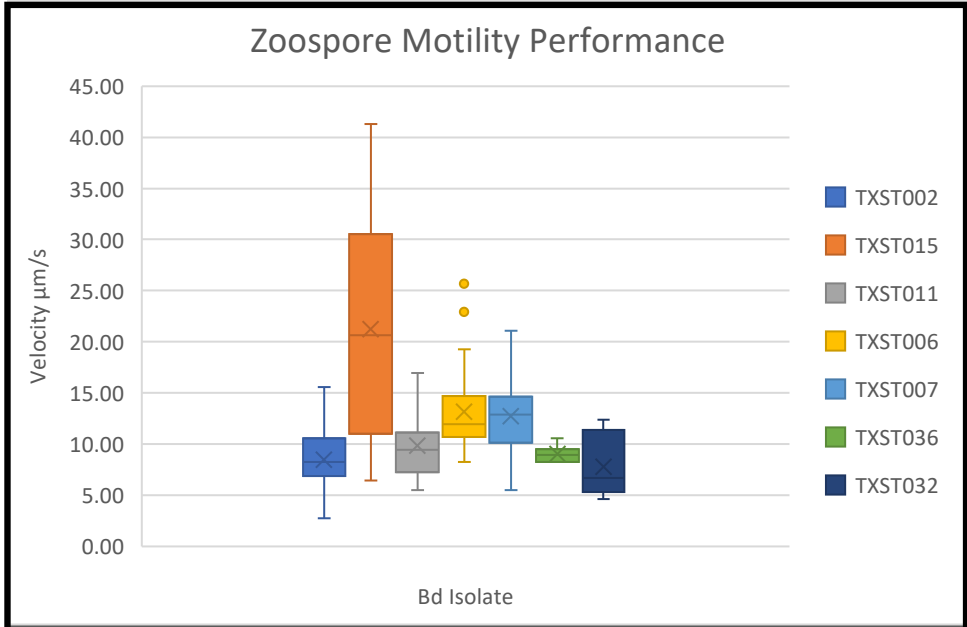


**Figure 4.** This box plot indicates zoospore motility performance in  $\mu\text{m/s}$  with TXST015 being the fastest and TXST002 being the slowest.

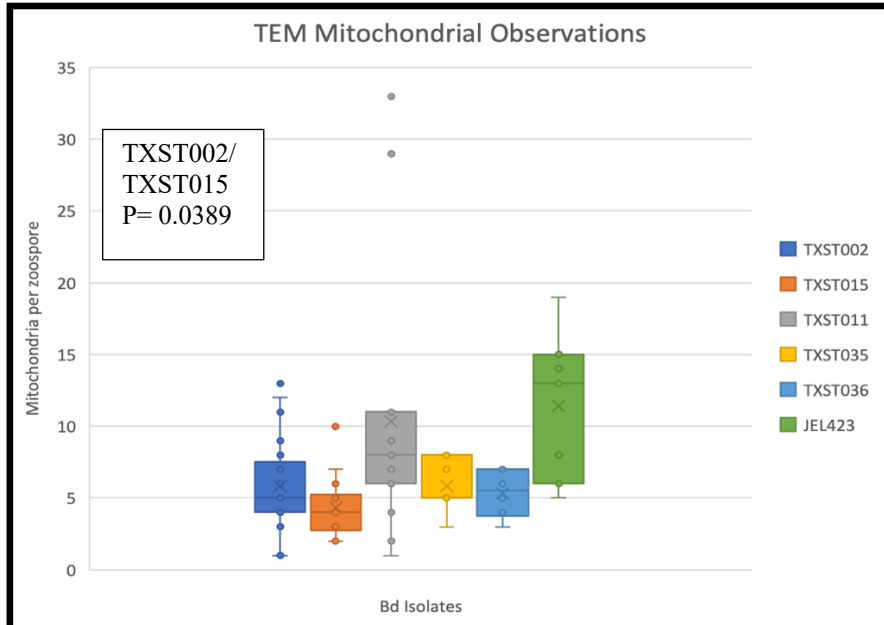


Figure 5. This box plot of TEM observations of mitochondria in Bd zoospores indicates that the greatest variation in the number of mitochondria observed was in TXST011 which had the instances of both greatest and least.

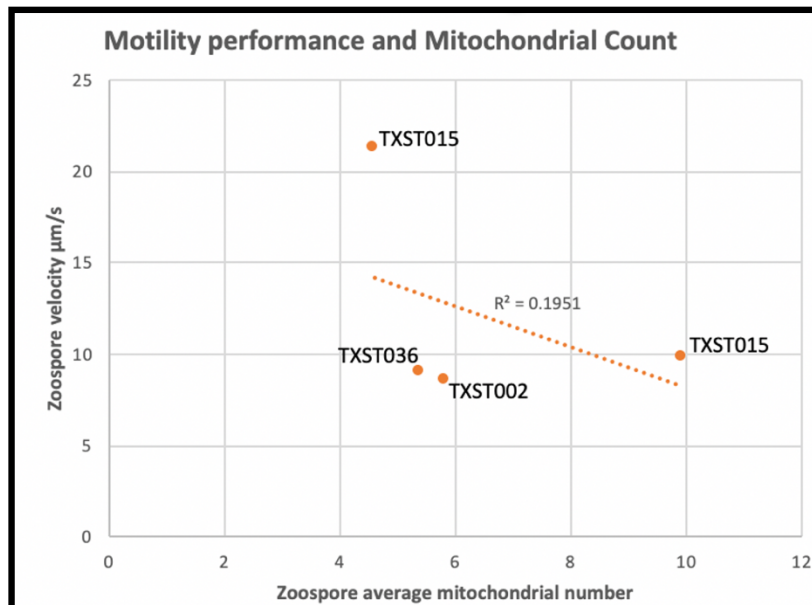
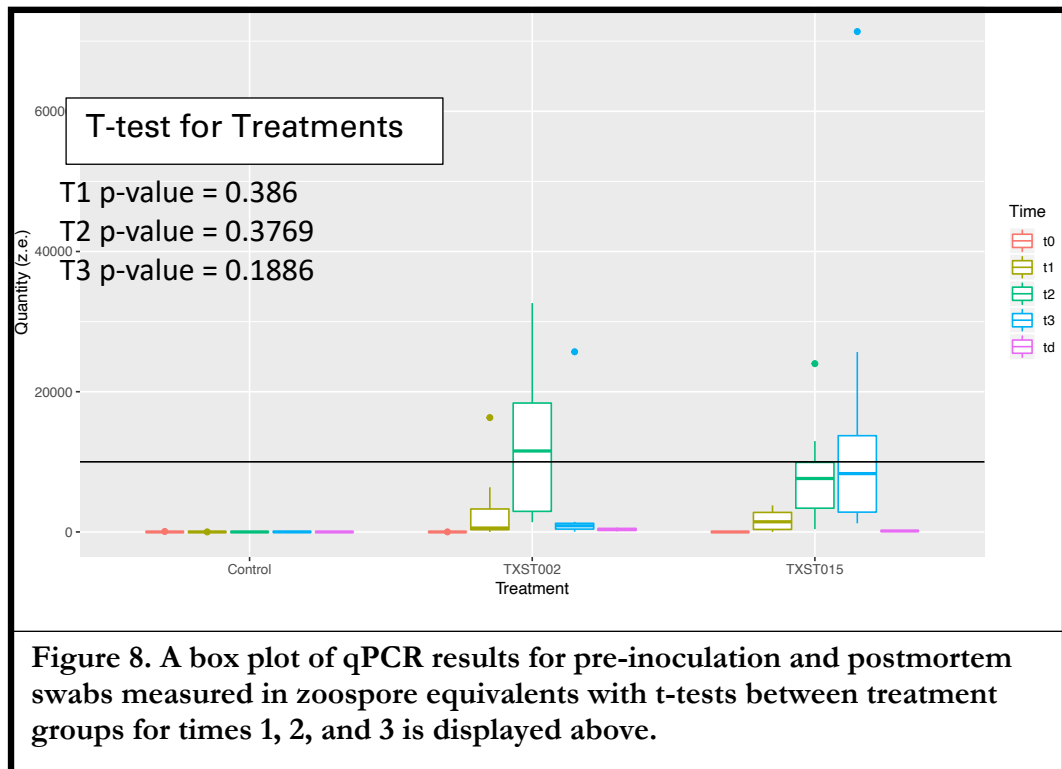
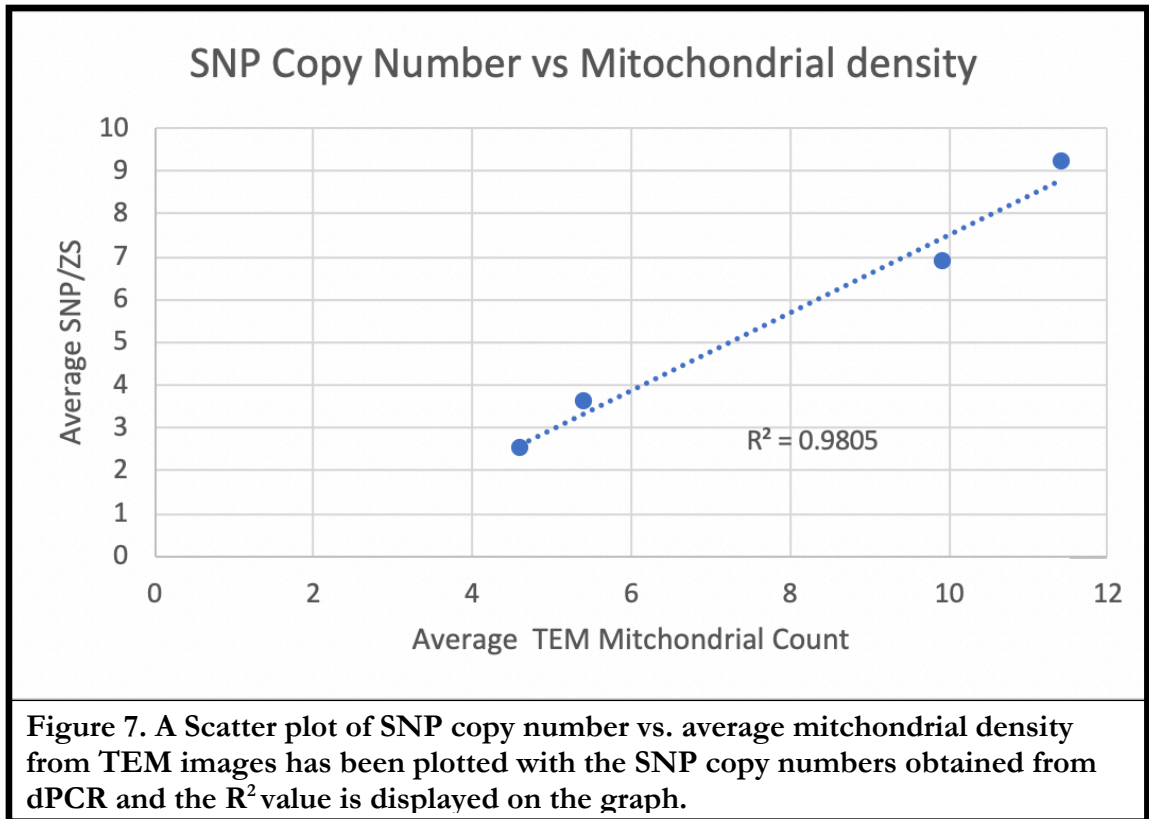


Figure 6. A Scatter plot of zoospore motility vs TEM mitochondrial observations does not indicate any correlation between the two variables.



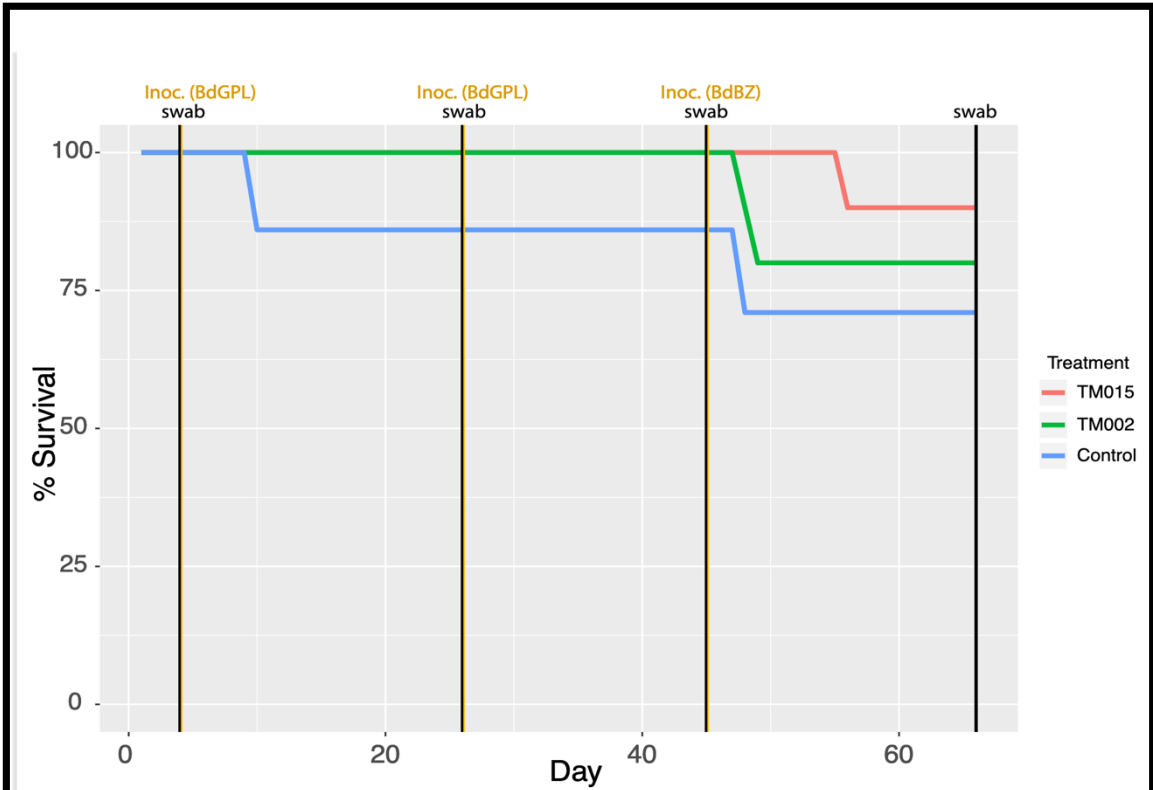
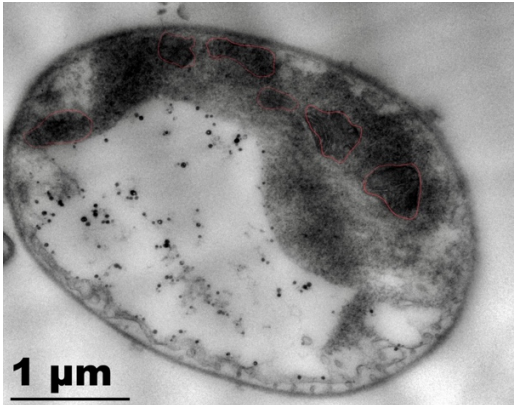
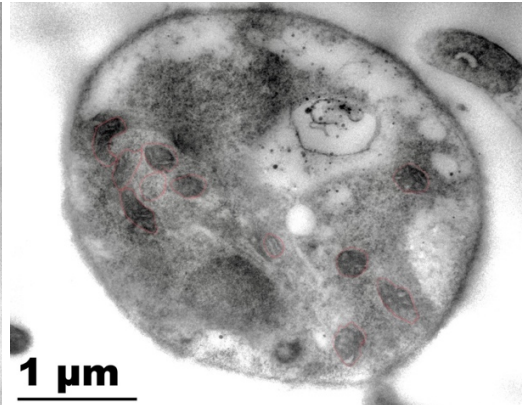


Figure 9. The mortality curve for the *Acris crepitans* infection experiment is flat with no indication of increased mortality due to the presence of a pathogen.



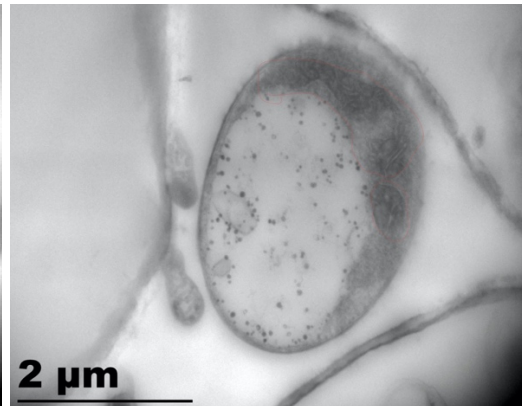
TXST011\_020



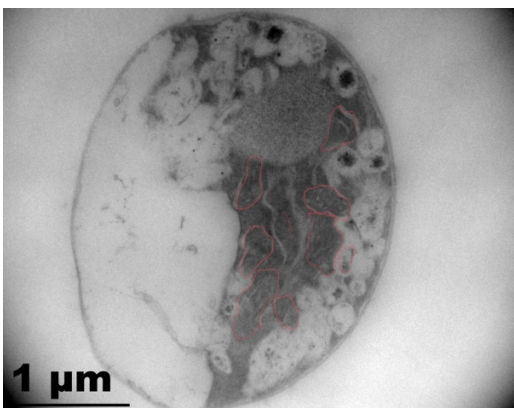
TXST011\_024



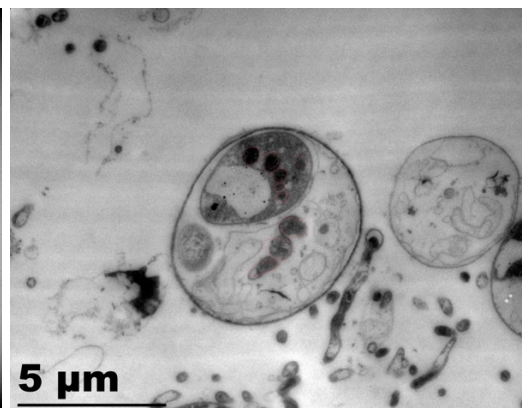
TXST011\_05



TXST011\_008

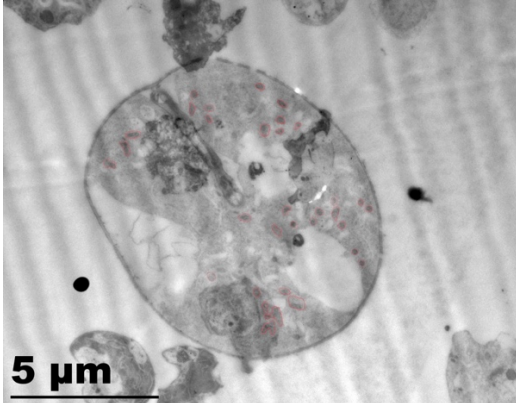


TXST011\_017

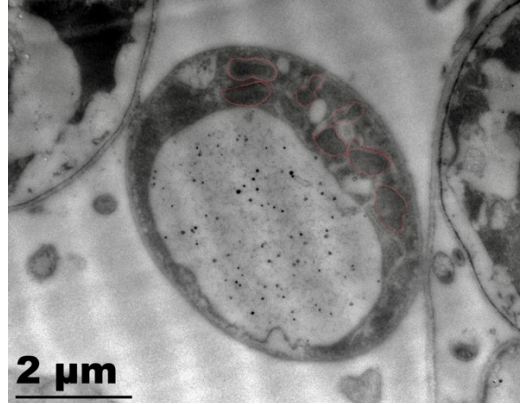


TXST011\_021

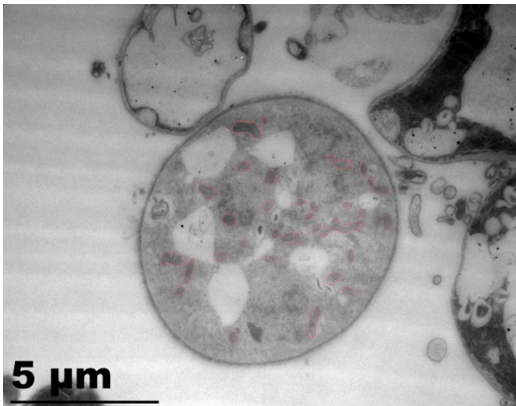
**Figure 10. TEM Micrographs of *Bd* Zoospores with scale bar in the lower left corner and mitochondria circled in red are labeled with isolate identification number followed by an underscore and a number which corresponds to the original image file.**



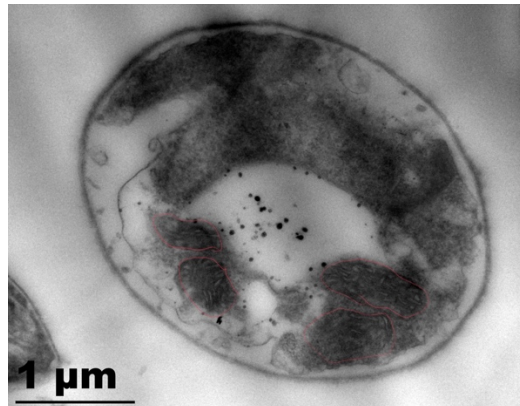
TXST011\_033



TXST011\_030



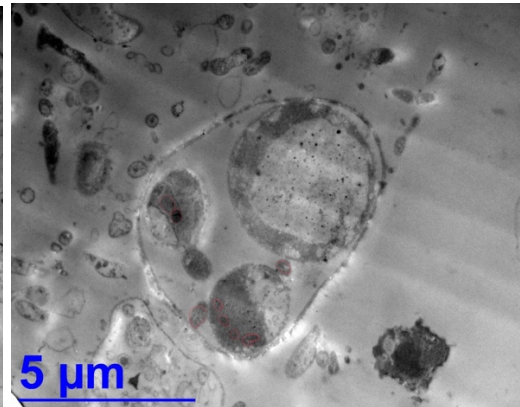
TXST011\_033



TXST011\_038

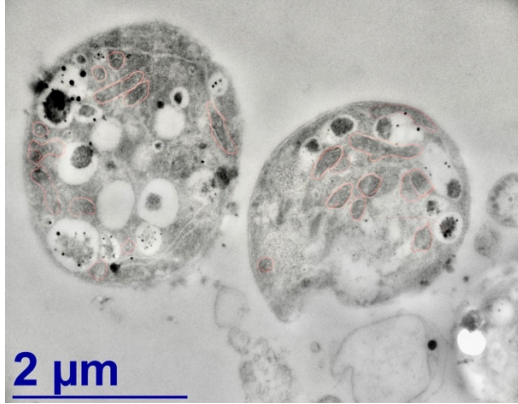


TXST011\_040



TXST011\_045

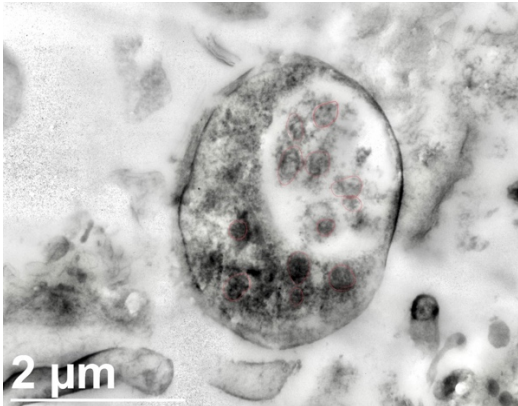
**Figure 10. Continued**



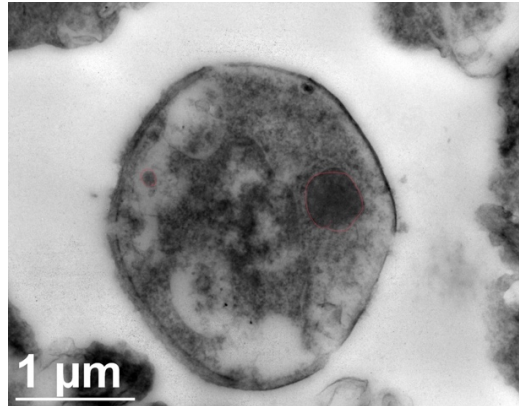
TXST011\_050



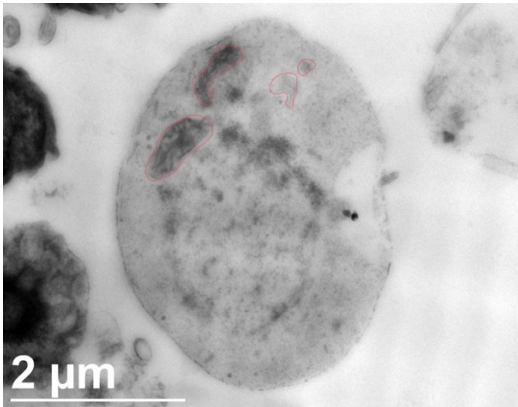
TXST011\_052



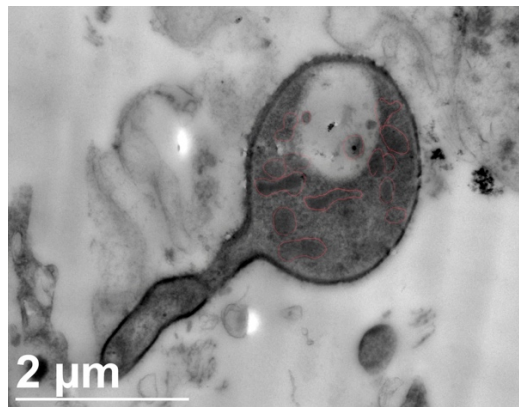
TXST002\_004



TXST002\_005

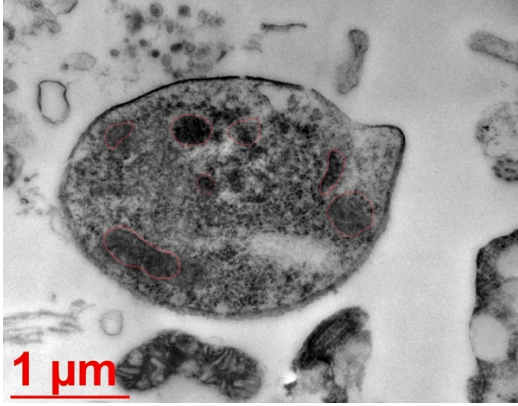


TXST002\_012



TXST002\_014

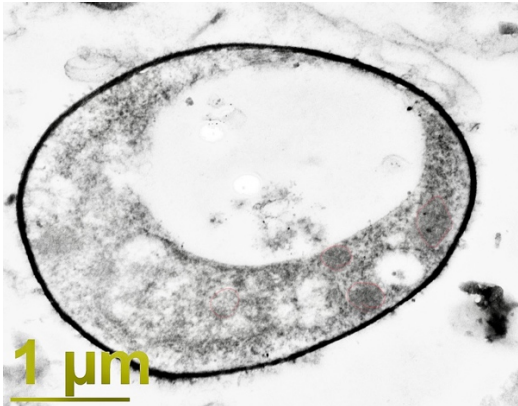
**Figure 10. Continued**



TXST002\_017



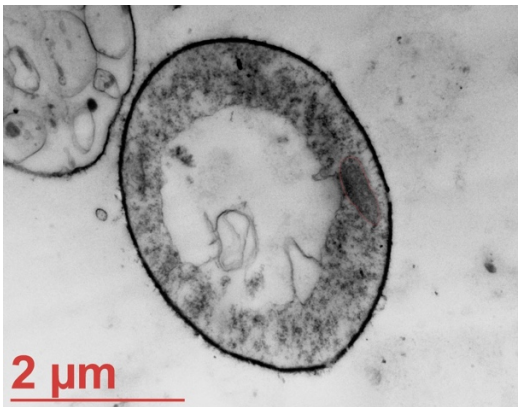
TXST002\_019



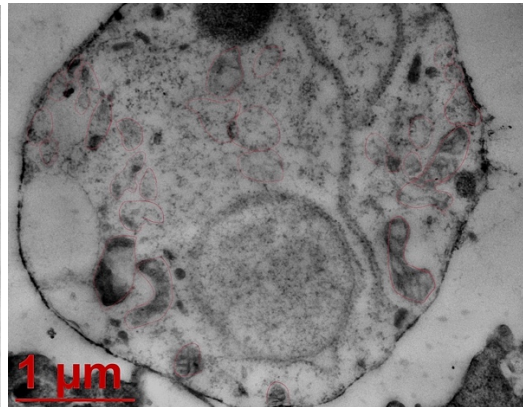
TXST002\_025



TXST002\_032

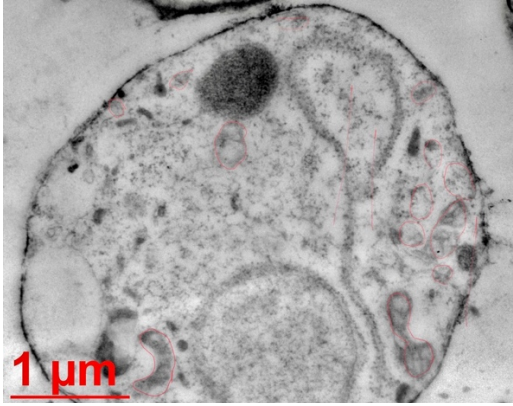


TXST002\_033



TXST002\_037

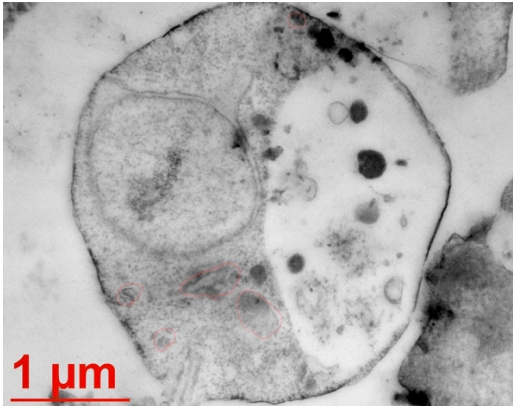
**Figure 10. Continued**



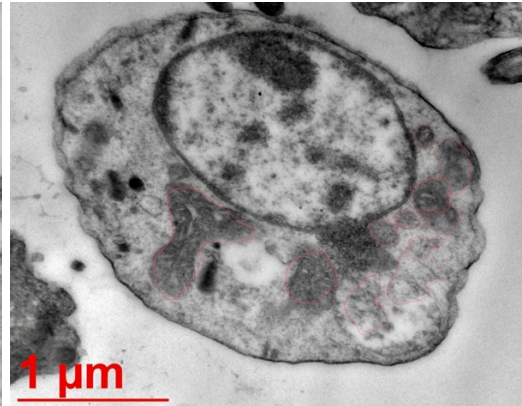
TXST002\_036



TXST002\_038



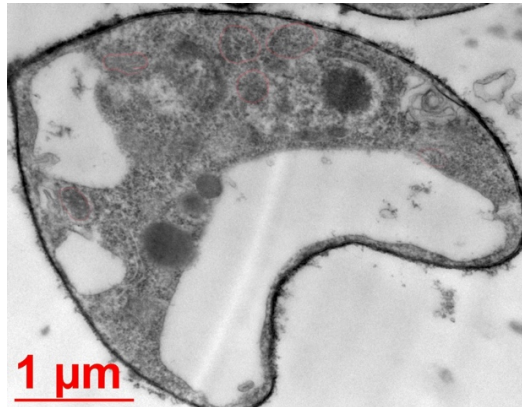
TXST002\_041



TXST002\_065

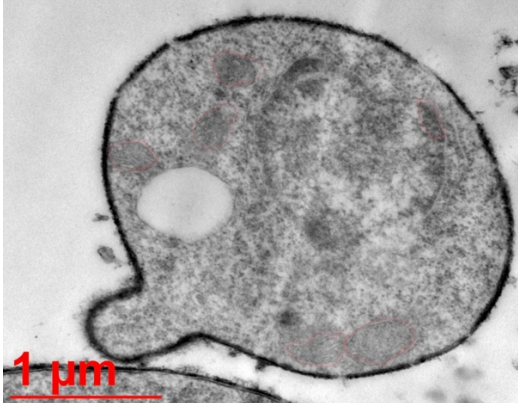


TXST002\_068

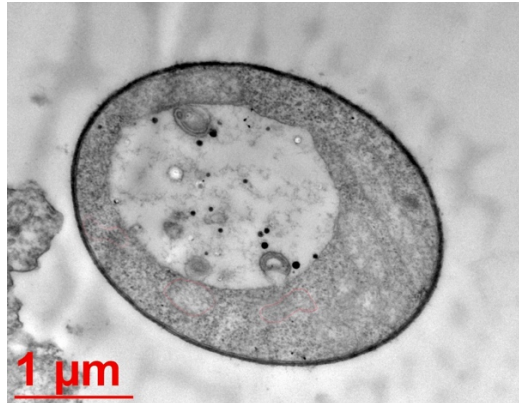


TXST002\_075

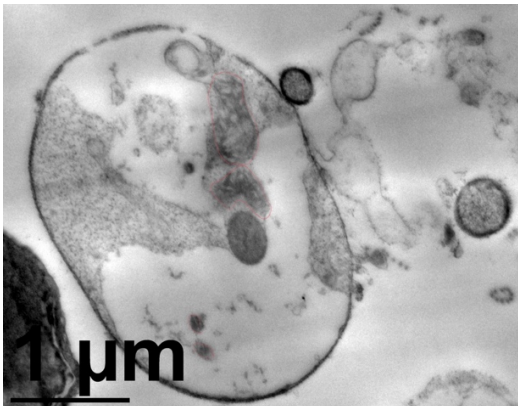
**Figure 10. Continued**



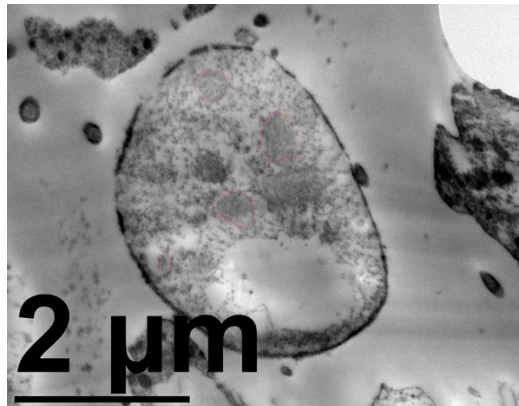
TXST002\_077



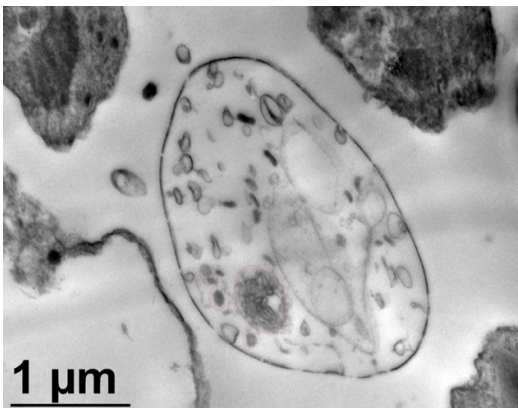
TXST002\_057



TXST002\_108



TXST002\_110

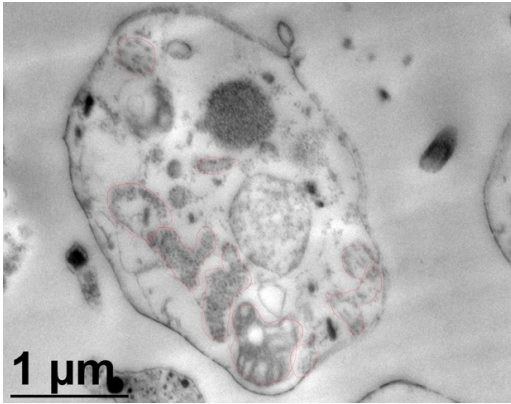


TXST002\_112

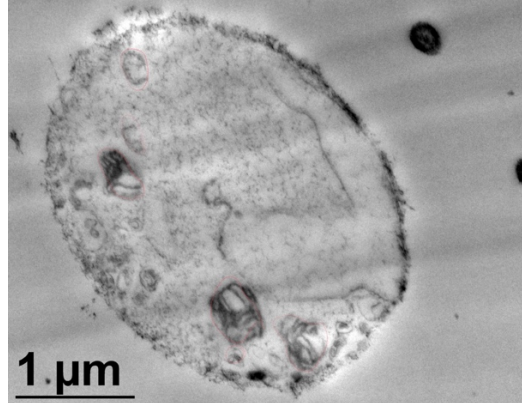


TXST002\_114

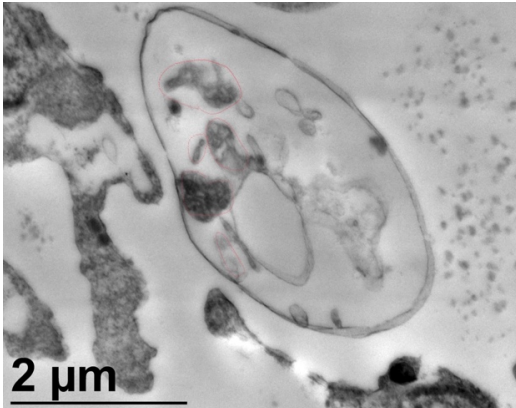
**Figure 10. Continued**



TXST002\_115



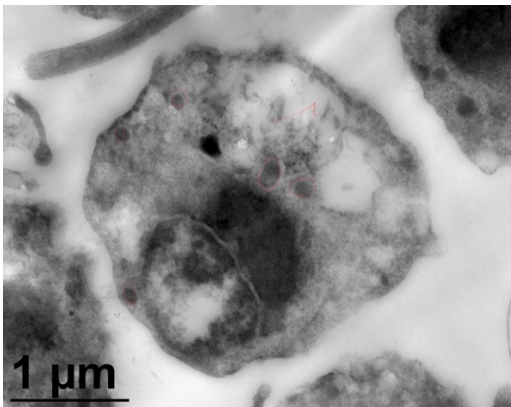
TXST002\_116



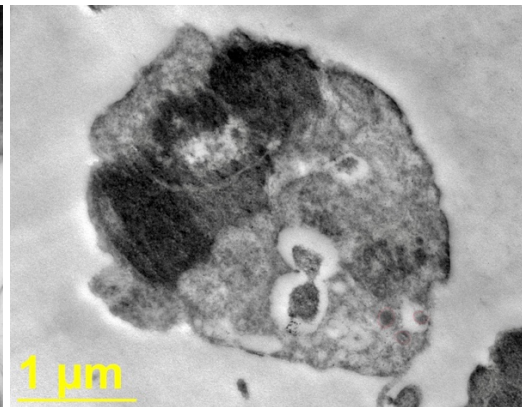
TXST002\_117



TXST002\_118

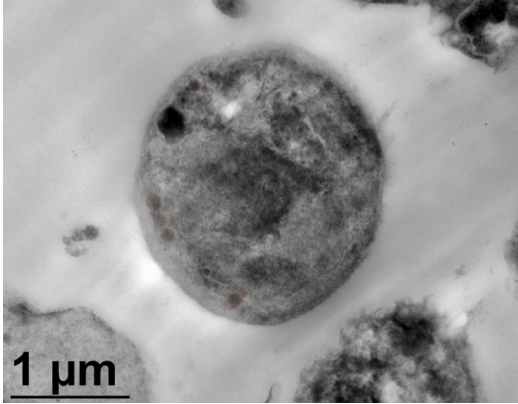


TXST015\_040

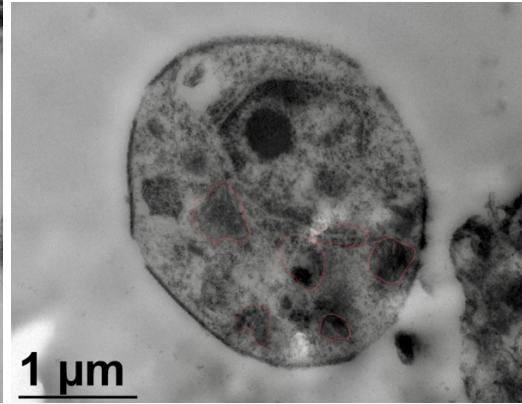


TXST015\_005

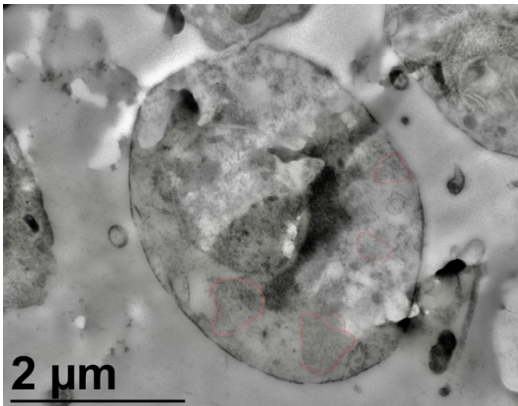
**Figure 10. Continued**



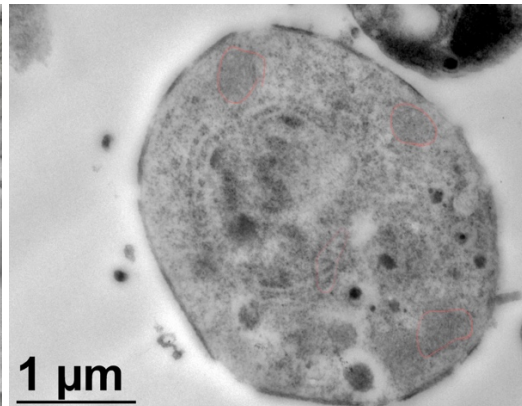
TXST015\_048



TXST015\_019



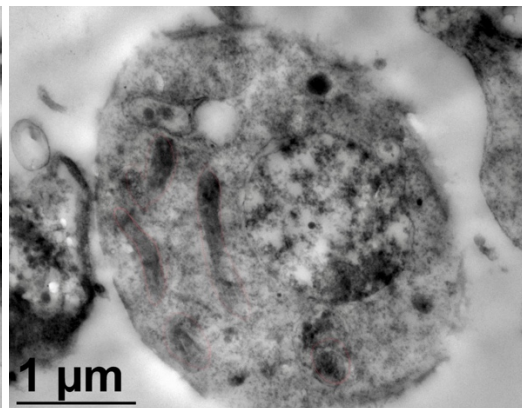
TXST015\_018



TXST015\_027

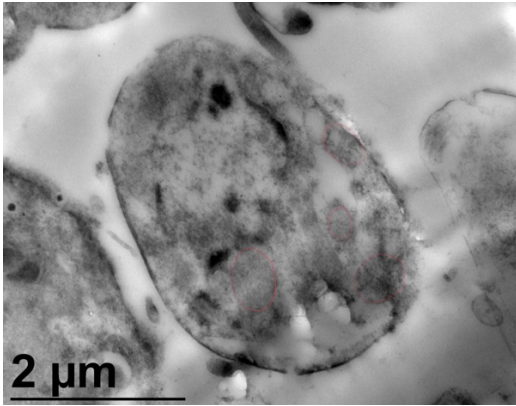


TXST015\_025

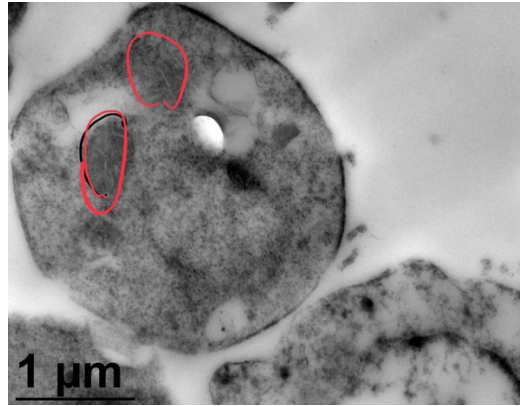


TXST015\_024

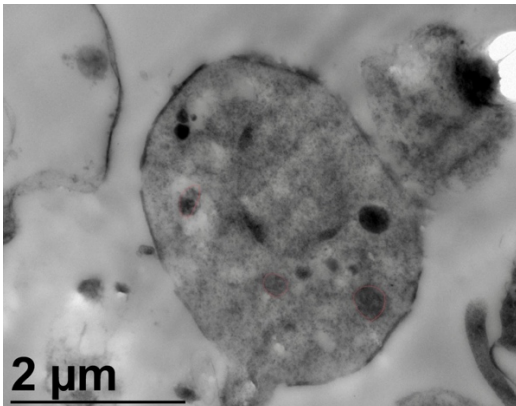
**Figure 10. Continued**



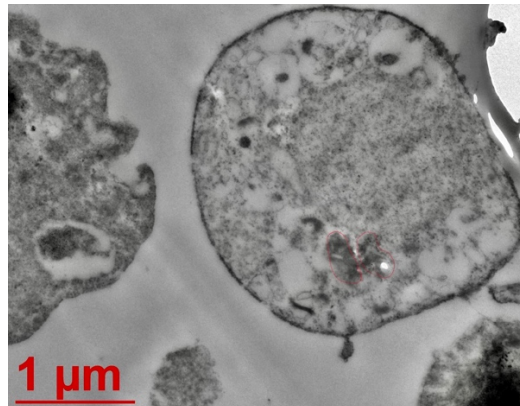
TXST015\_028



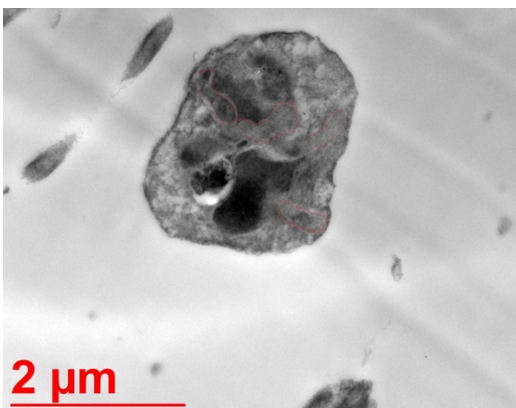
TXST015\_030



TXST015\_032



TXST015\_056



TXST015\_068

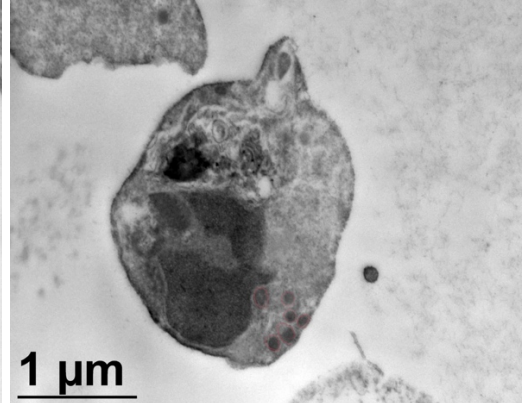


TXST015\_074

**Figure 10. Continued**



TXST015\_077



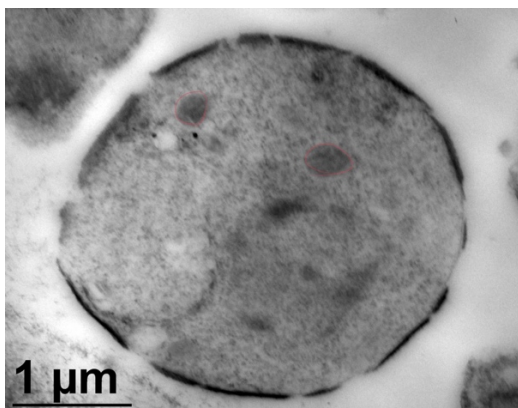
TXST015\_079



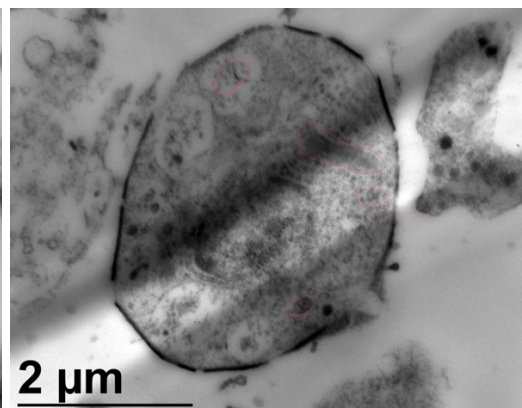
TXST015\_091



TXST015\_094

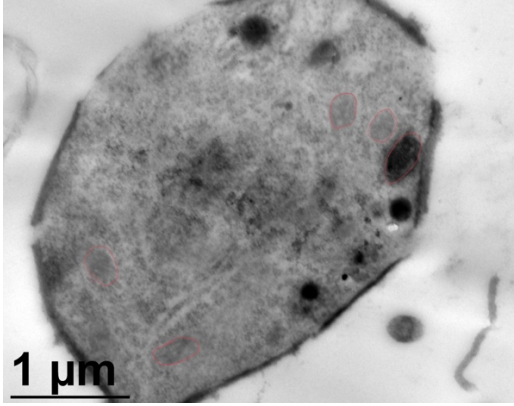


TXST015\_096

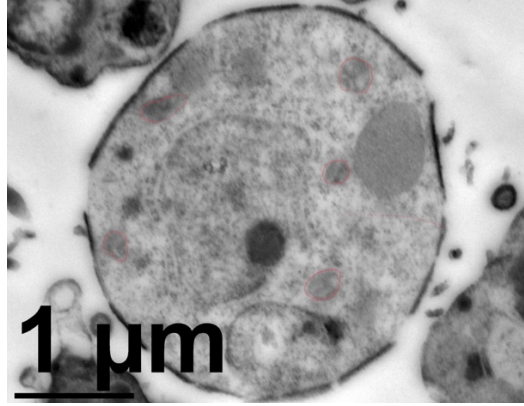


TXST015\_098

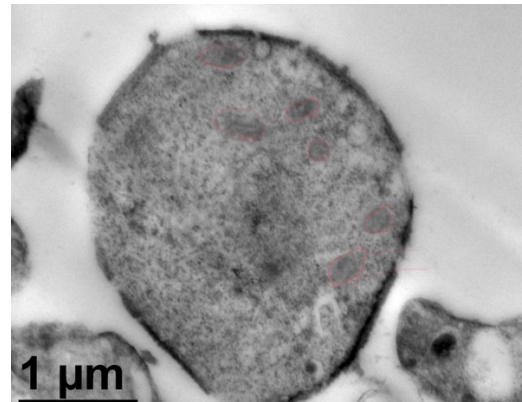
**Figure 10. Continued**



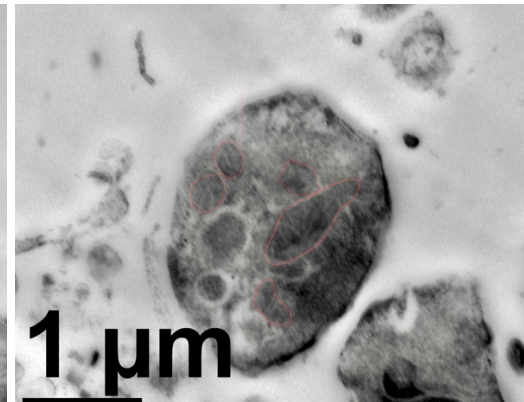
TXST015\_099



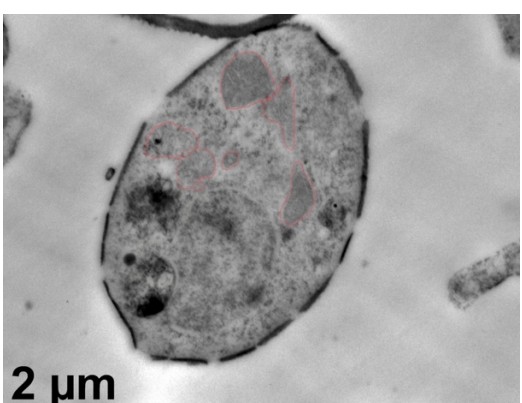
TXST015\_100



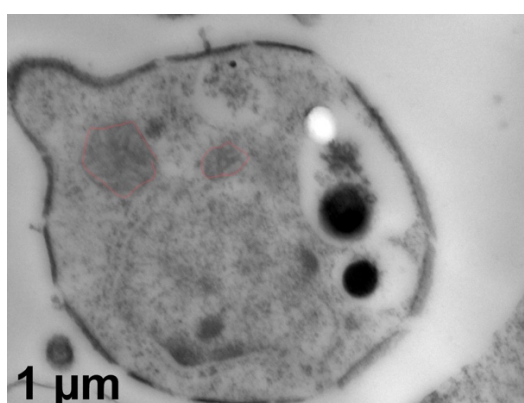
TXST015\_103



TXST015\_104



TXST015\_107

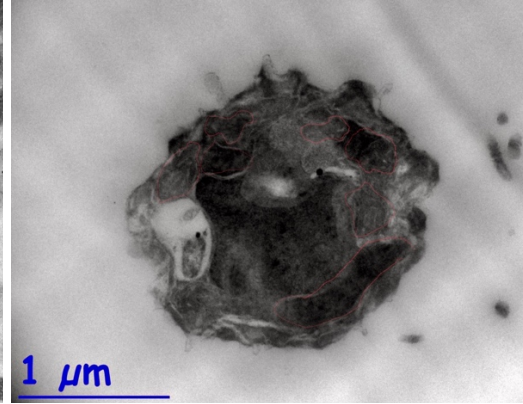


TXST015\_109

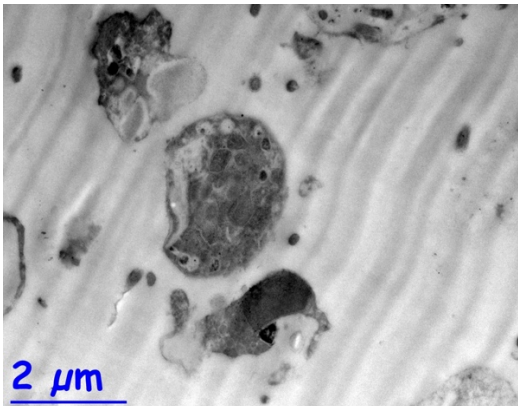
Figure 10. Continued



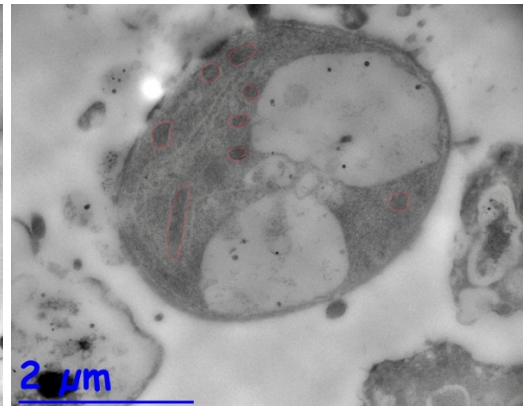
TXST035\_012



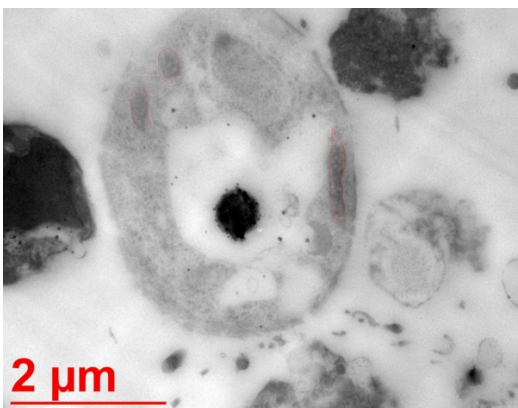
TXST035\_032



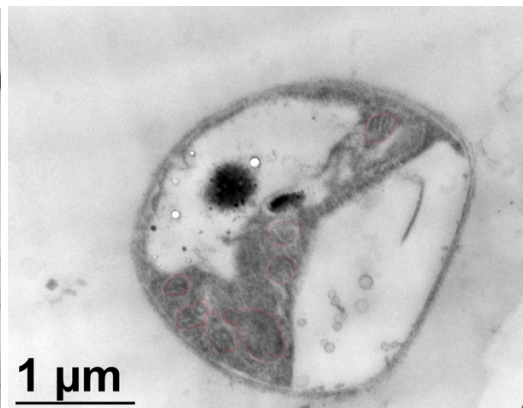
TXST035\_025



TXST035\_030

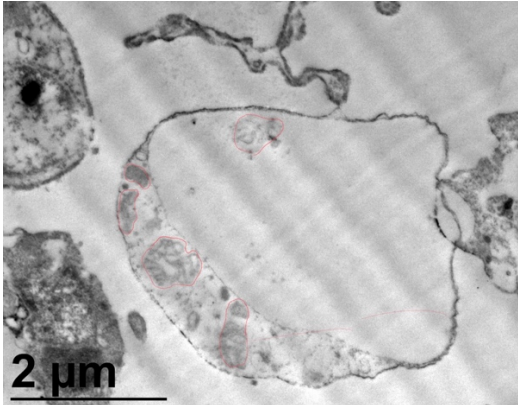


TXST035\_042

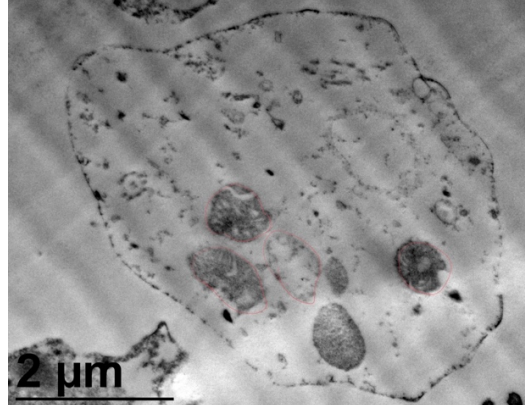


TXST035\_050

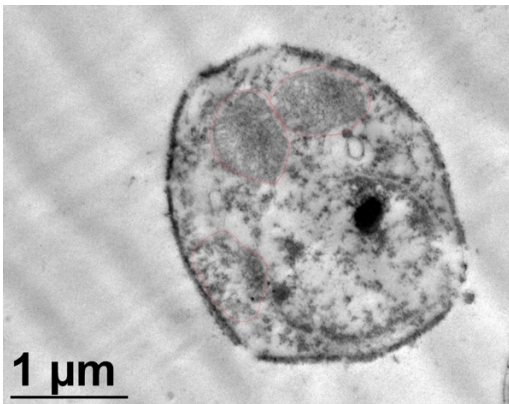
**Figure 10. Continued**



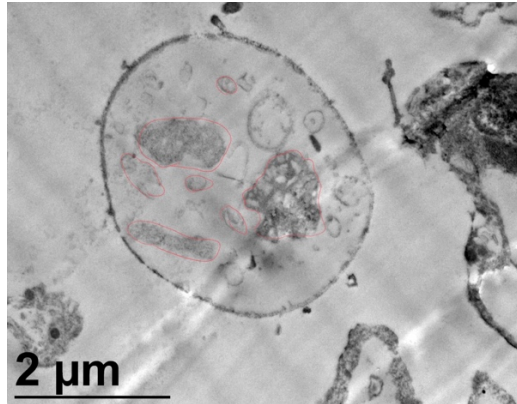
TXST036\_019



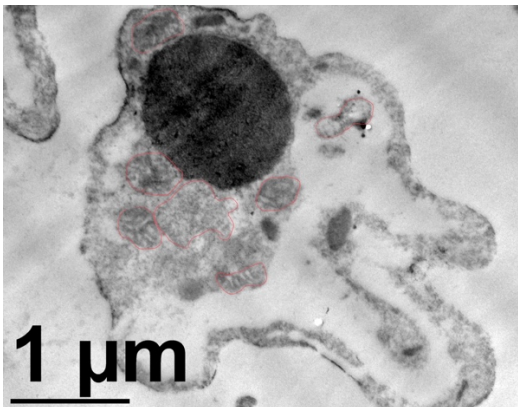
TXST036\_020



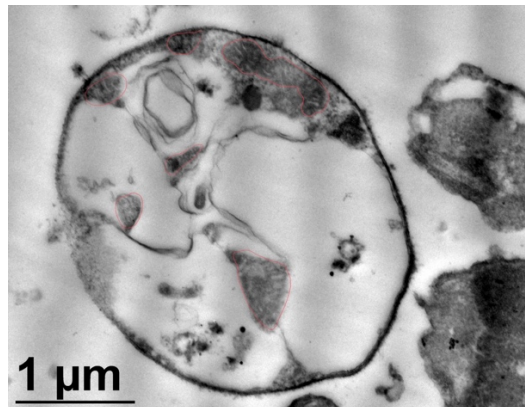
TXST036\_021



TXST036\_023

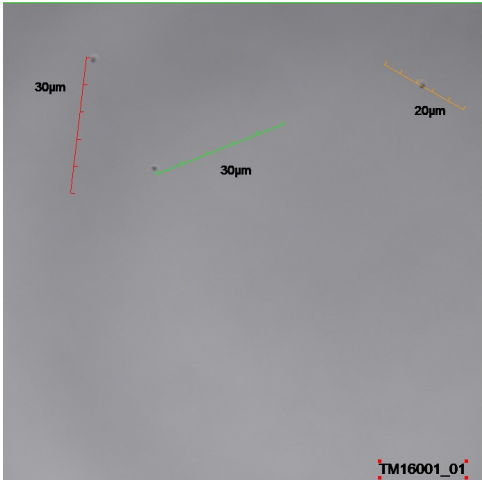


TXST036\_024

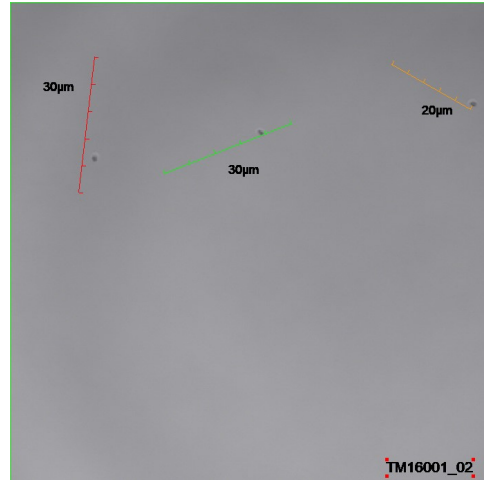


TXST036\_029

**Figure 10. Continued**



TXST002\_1\_1



TXST002\_1\_2



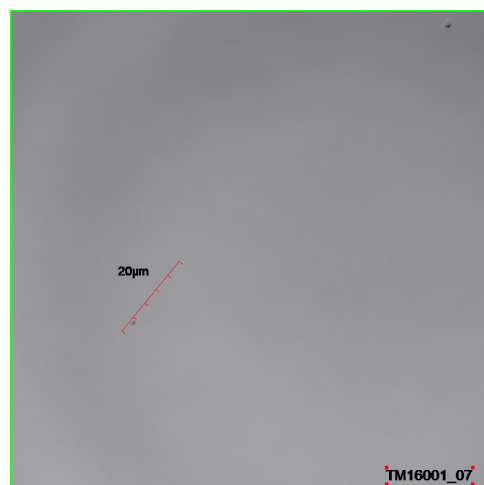
TXST002\_1\_3



TXST002\_1\_4



TXST002\_1\_06



TXST002\_1\_07

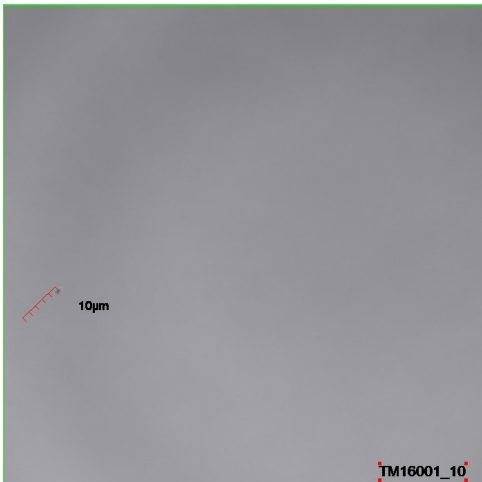
**Figure 11. A confocal time series of micrographs of live *Bd* zoospores which are identified by isolate\_image file name\_sequence number are displayed above.**



TXST002\_1\_8



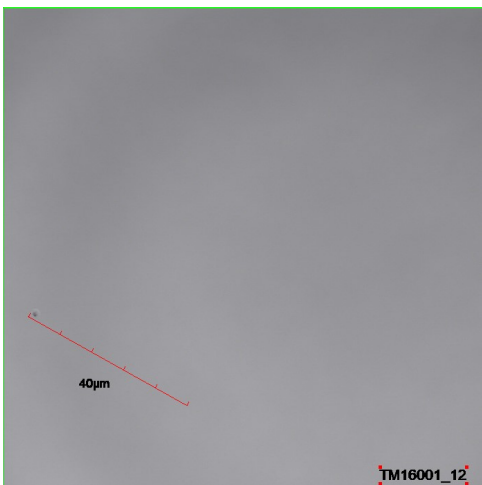
TXST002\_1\_9



TXST002\_1\_10



TXST002\_1\_11

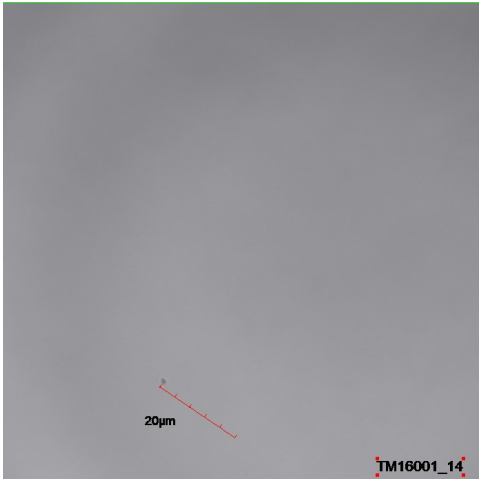


TXST015\_1\_12



TXST015\_1\_013

**Figure 11. Continued**



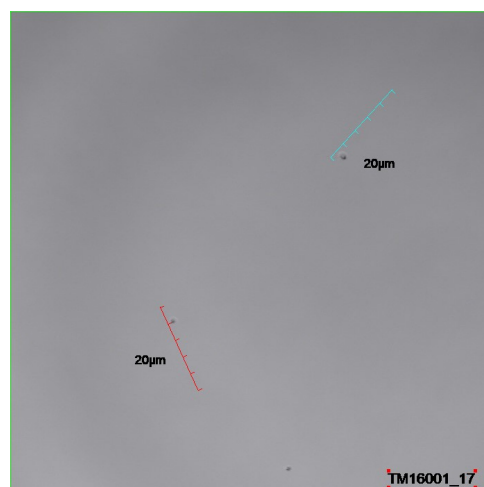
TXST002\_1\_14



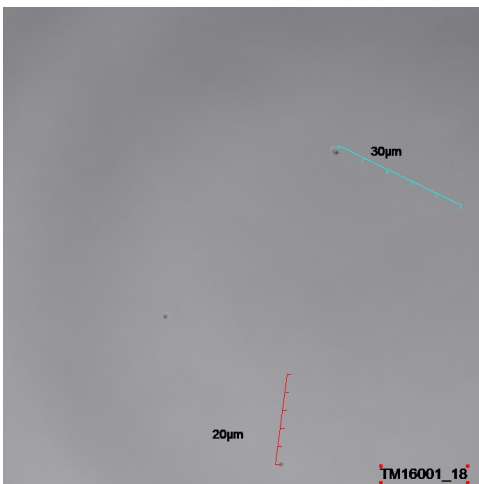
TXST002\_1\_15



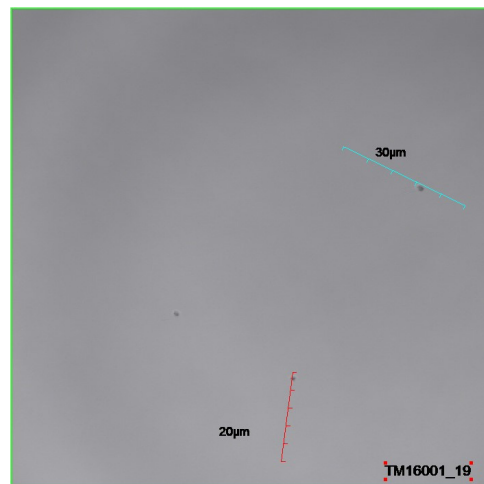
TXST002\_1\_16



TXST002\_1\_17



TXST002\_1\_08



TXST002\_1\_19

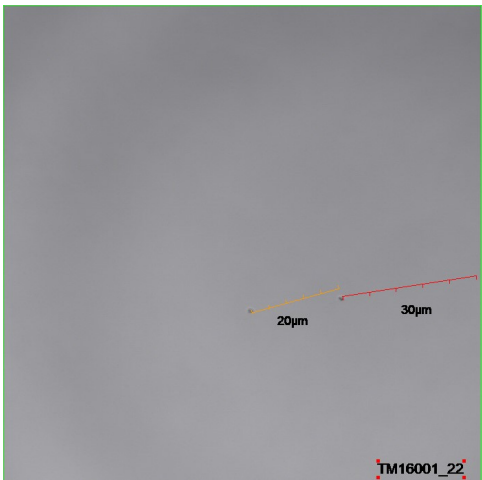
**Figure 11. Continued**



TXST002\_1\_20



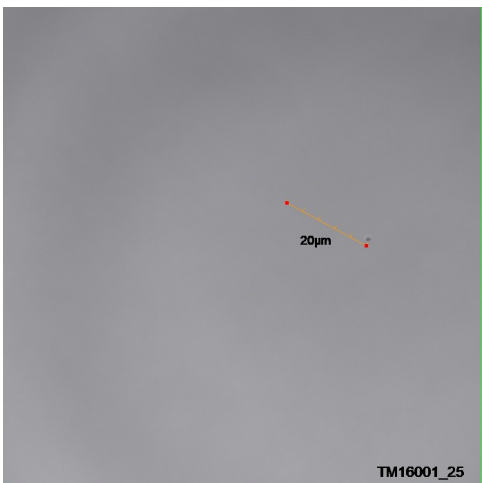
TXST002\_1\_21



TXST002\_1\_22



TXST002\_1\_023

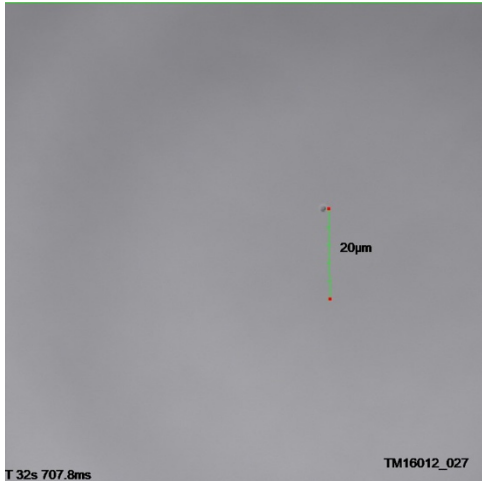


TXST002\_1\_025

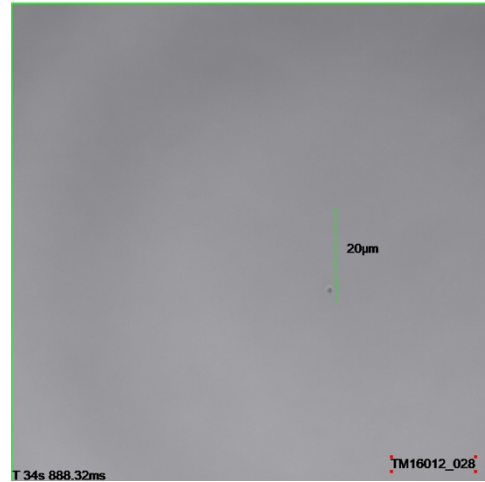


TXST002\_1\_026

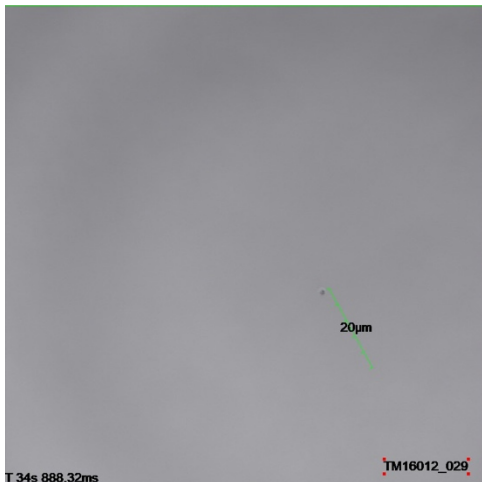
**Figure 11. Continued**



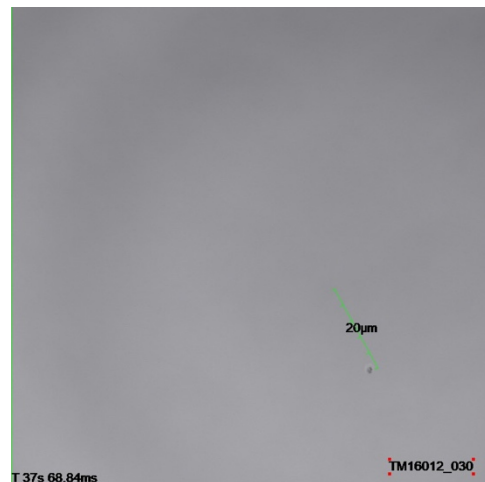
TXST002\_12\_027



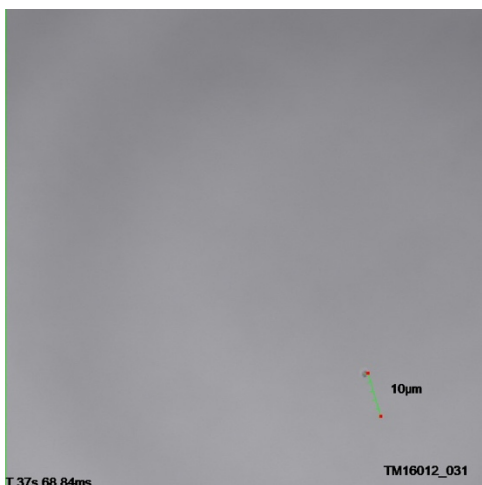
TXST002\_12\_028



TXST002\_12\_029



TXST002\_12\_030

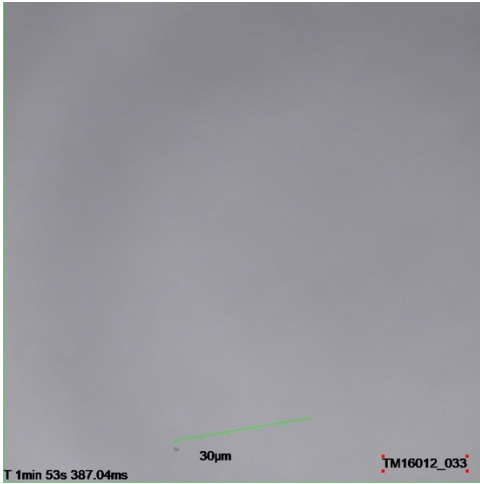


TXST002\_12\_031



TXST002\_12\_032

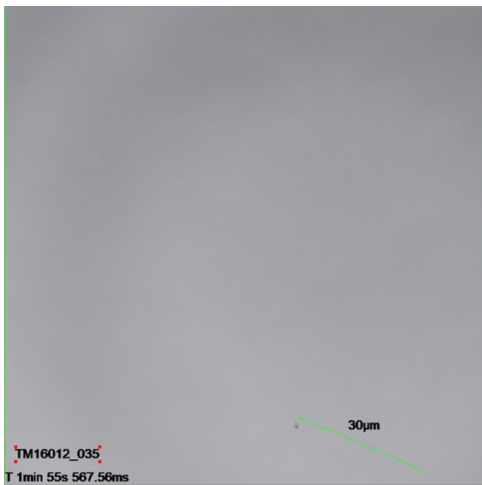
**Figure 11. Continued**



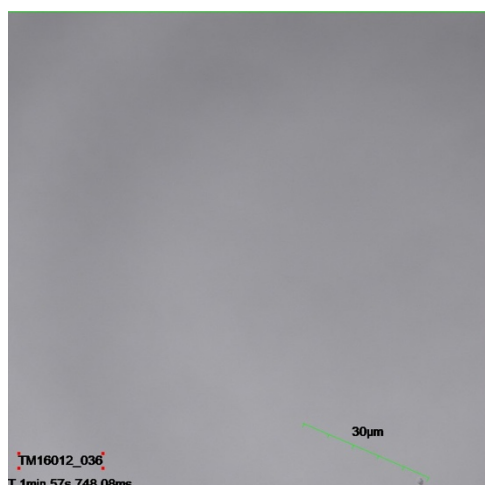
TXST002\_12\_033



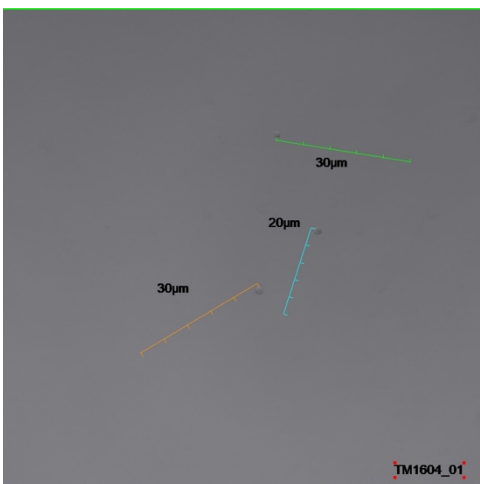
TXST002\_12\_034



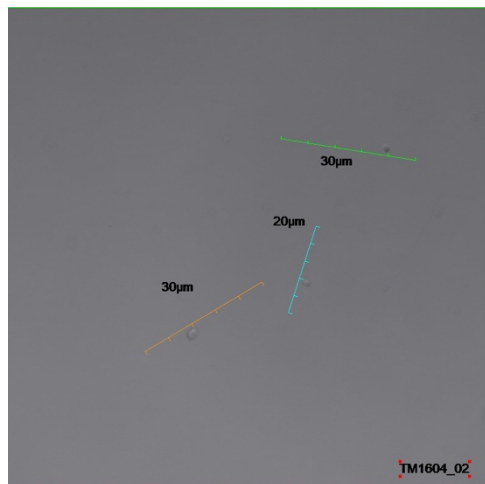
TXST002\_12\_035



TXST002\_12\_036



TXST002\_4\_1



TXST002\_4\_2

Figure 11. Continued



TXST002\_4\_3



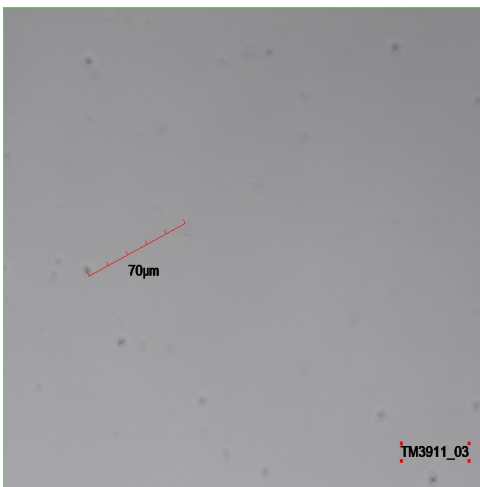
TXST002\_4\_4



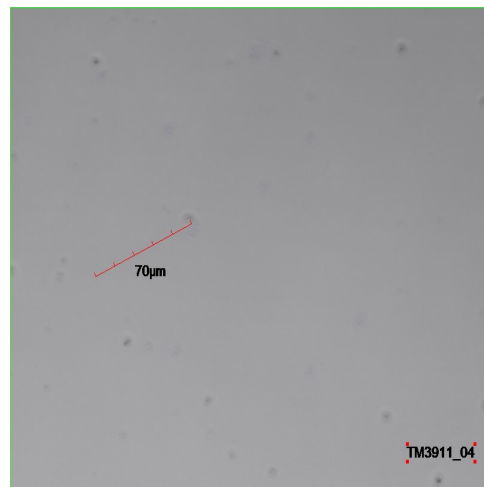
TXST015\_11\_1



TXST015\_11\_2

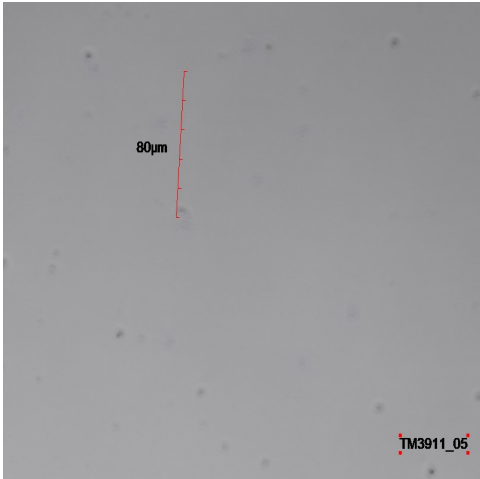


TXST015\_11\_3

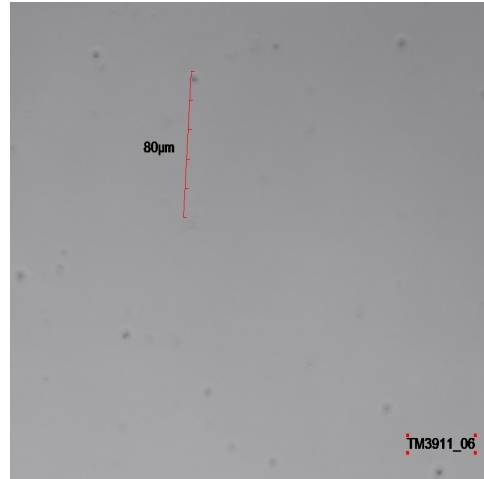


TXST015\_11\_04

**Figure 11. Continued**



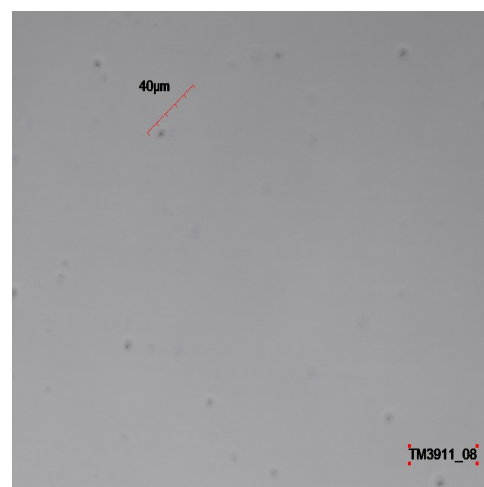
TXST015\_11\_5



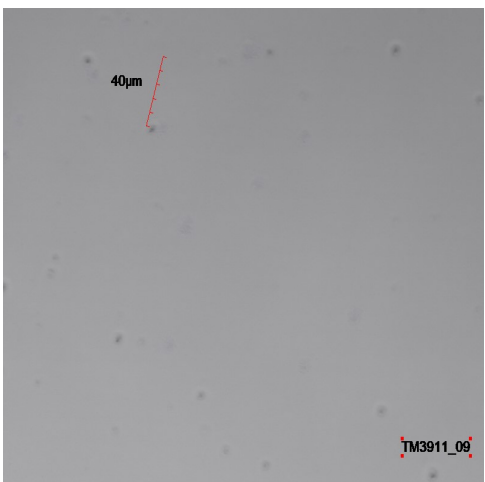
TXST015\_11\_6



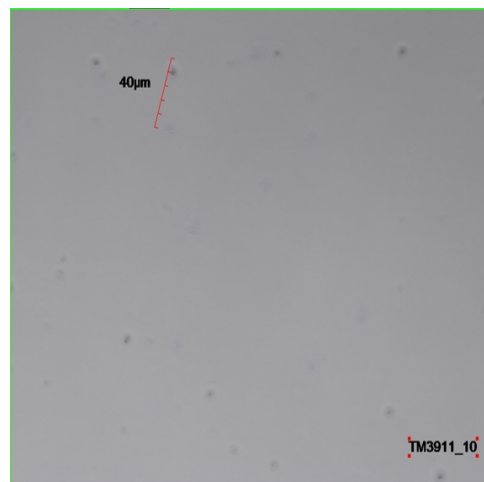
TXST015\_11\_7



TXST015\_11\_8

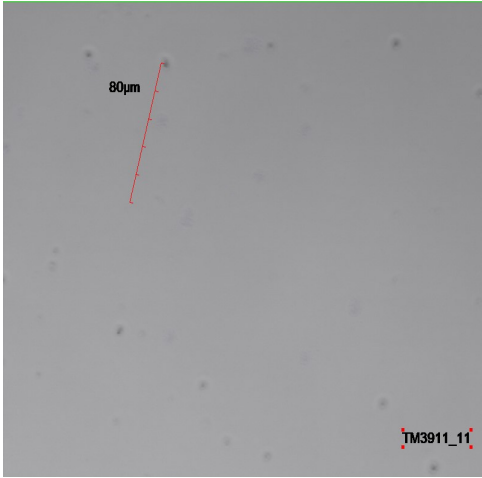


TXST015\_11\_9

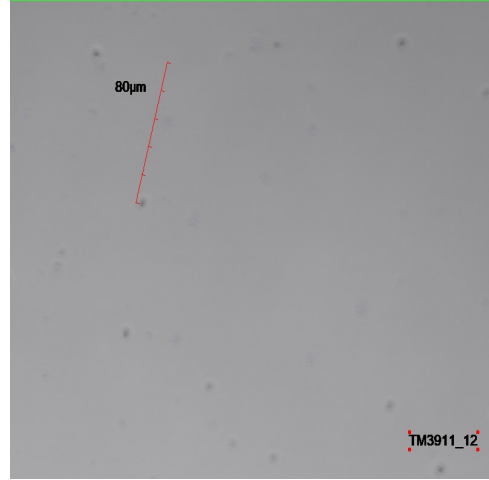


TXST015\_11\_10

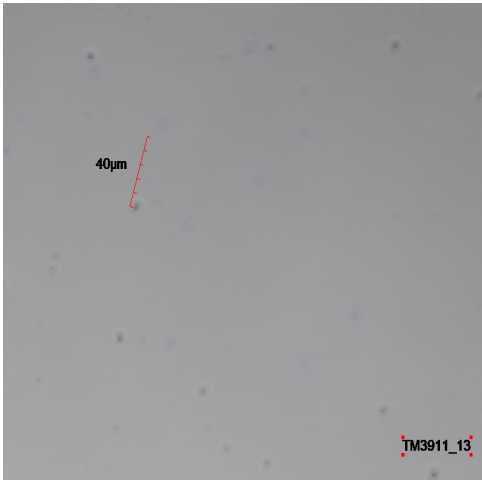
**Figure 11. Continued**



TXST015\_11\_11



TXST015\_11\_12



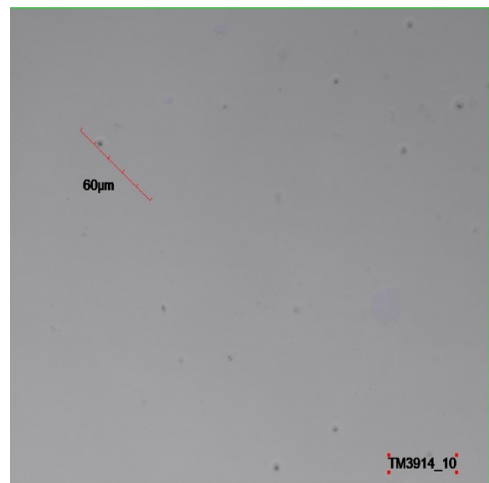
TXST015\_11\_13



TXST015\_11\_14

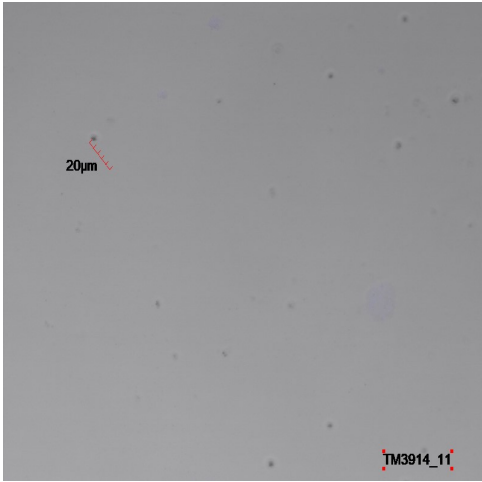


TXST015\_14\_9



TXST015\_14\_10

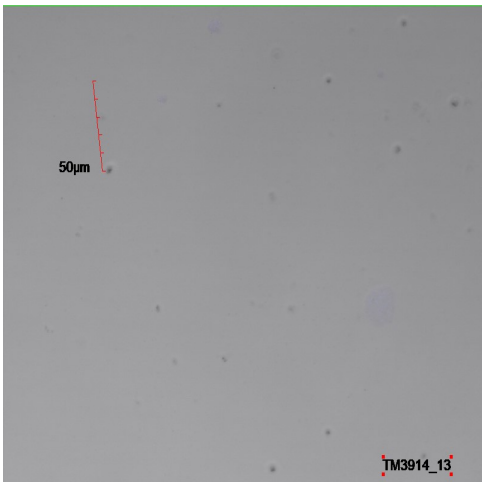
**Figure 11. Continued**



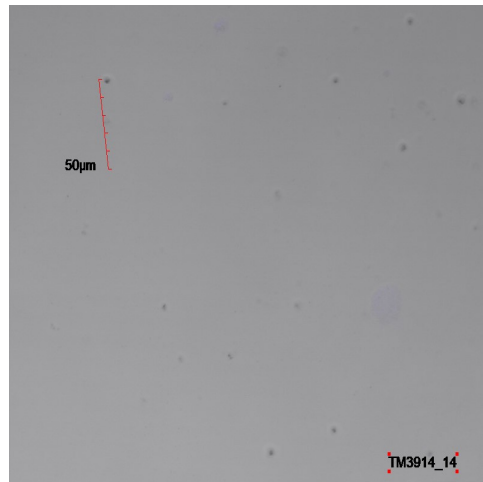
TXST015\_14\_11



TXST015\_14\_12



TXST015\_14\_13



TXST015\_14\_14

**Figure 11. Continued**

## LITERATURE CITED

- Becker, C. G., et al. (2017). "Variation in phenotype and virulence among enzootic and panzootic amphibian chytrid lineages." Fungal Ecology **26**: 45-50.
- Berger, L., et al. (2005). "Life cycle stages of the amphibian chytrid *Batrachochytrium dendrobatidis*." Dis Aquat Organ **68**(1): 51-63.
- Berger, L., et al. (2005). "Virulence of the amphibian chytrid fungus *Batrachochytrium dendrobatidis* varies with the strain." Dis Aquat Organ **68**(1): 47-50.
- Berger, L., et al. (1998). "Chytridiomycosis causes amphibian mortality associated with population declines in the rain forests of Australia and Central America." Proc Natl Acad Sci U S A **95**(15): 9031-9036.
- Blaustein, A. and J. M. Kiesecker (2002). "Complexity in conservation: Lessons from the global decline of amphibian populations." Ecology Letters **5**: 597-608.
- Boyle, D. G., et al. (2004). "Rapid quantitative detection of chytridiomycosis (*Batrachochytrium dendrobatidis*) in amphibian samples using real-time Taqman PCR assay." Dis Aquat Organ **60**(2): 141-148.
- Daszak, P., et al. (2000). "Emerging infectious diseases of wildlife--threats to biodiversity and human health." Science **287**(5452): 443-449.
- DePaula and Catão-Dias (2011). "Chytridiomycosis: a Devastating Emerging Fungal Disease of Amphibians " Brazilian Journal of Veterinary Pathology **4**: 250-258.
- E Smith, M., et al. (2008). "Intra-specific and intra-sporocarp ITS variation of ectomycorrhizal fungi as assessed by rDNA sequencing of sporocarps and pooled ectomycorrhizal roots from a *Quercus* woodland." Mycorrhiza **18**: 15-22.
- Houlahan, J. E., et al. (2000). "Quantitative evidence for global amphibian population declines." Nature **404**(6779): 752-755.
- Jenkinson, T. S., et al. (2018). "Globally invasive genotypes of the amphibian chytrid outcompete an enzootic lineage in coinfections." Proc Biol Sci **285**(1893): 20181894.
- Kolby, J. E. and P. Daszak (2016). "The Emerging Amphibian Fungal Disease, Chytridiomycosis: A Key Example of the Global Phenomenon of Wildlife Emerging Infectious Diseases." Microbiol Spectr **4**(3).
- Lam, B. A., et al. (2011). "Motile zoospores of *Batrachochytrium dendrobatidis* move away from antifungal metabolites produced by amphibian skin bacteria." EcoHealth **8**(1): 36-45.

- Lehtinen, R. M. and M. C. MacDonald (2011). "Live Fast Die Young? A Six-Year Field study of Survivorship in Blanchard's Cricket Frog (*Acris crepitans blanchardi*)."  
Herpetological Review(4): 504-507.
- Longcore, J., et al. (1999). "Batrachochytrium Dendrobatidis gen. et sp. nov., a Chytrid Pathogenic to Amphibians." Mycologia **91**: 219.
- Longo, A. V., et al. (2013). "ITS1 copy number varies among Batrachochytrium dendrobatidis strains: implications for qPCR estimates of infection intensity from field-collected amphibian skin swabs." PLoS One **8**(3): e59499.
- Marshall, T., et al. (2019). "Genetic characterization of chytrids isolated from larval amphibians collected in central and east Texas." Fungal Ecology **39**: 55-62.
- Moss, A. S., et al. (2008). "Chemotaxis of the amphibian pathogen Batrachochytrium dendrobatidis and its response to a variety of attractants." Mycologia **100**(1): 1-5.
- Olson, D. H., et al. (2013). "Mapping the global emergence of Batrachochytrium dendrobatidis, the amphibian chytrid fungus." PLoS One **8**(2): e56802.
- Piotrowski, J. S., et al. (2004). "Physiology of Batrachochytrium dendrobatidis, a chytrid pathogen of amphibians." Mycologia **96**(1): 9-15.
- Rebollar, E. A., et al. (2017). "Prevalence and pathogen load estimates for the fungus Batrachochytrium dendrobatidis are impacted by ITS DNA copy number variation." Dis Aquat Organ **123**(3): 213-226.
- Rodriguez, D., et al. (2014). "Long-term endemism of two highly divergent lineages of the amphibian-killing fungus in the Atlantic Forest of Brazil." Mol Ecol **23**(4): 774-787.
- Skerratt, L., et al. (2007). "Spread of Chytridiomycosis Has Caused the Rapid Global Decline and Extinction of Frogs." EcoHealth **4**: 125-134.
- Skerratt, L., et al. (2011). "Validation of Diagnostic Tests in Wildlife: The Case of Chytridiomycosis in Wild Amphibians." Journal of Herpetology **45**.
- Stuart, S., et al. (2005). "Status and Trends of Amphibian Declines and Extinctions Worldwide." Science (New York, N.Y.) **306**: 1783-1786.
- Voyles, J., et al. (2009). "Pathogenesis of chytridiomycosis, a cause of catastrophic amphibian declines." Science **326**(5952): 582-585.